$CD24^+$ liver tumor-initiating cells drive self-renewal and tumor initiation through Stat3-mediated Nanog regulation

Terence Kin Wah Lee[1,2], Antonia Castilho[1,2], Vincent Chi Ho Cheung [1,2], Kwan Ho Tang[2], Stephanie Ma[1,2], Irene Oi Lin Ng[1,2 #]

[1]State Key Laboratory for Liver Research, The University of Hong Kong,
[2]Liver Cancer and Hepatitis Research Laboratory, Department of Pathology,
Li Ka Shing Faculty of Medicine, The University of Hong Kong

[#]To whom correspondence should be addressed: Prof. Irene O.L. Ng, Room 127B, University Pathology Building, Department of Pathology, The University of Hong Kong, Queen Mary Hospital, Pokfulam, Hong Kong. Tel: (852) 2255-3967; Fax: (852) 2872-5197; Email: iolng@hku.hk.

Running title: $CD24^+$ cells drive self-renewal and tumor formation

Keywords: CD24; chemoresistance; Nanog; HCC; Stat3

Abbreviations: Tumor-initiating cells, T-IC; epithelial cell adhesion molecule, EpCAM; hepatocellular carcinoma, HCC; immunohistochemistry, IHC; quantitative PCR , qPCR.

Financial support: The study was supported by Hong Kong Research Grants Council Collaborative Research Fund (HKU 1/06C and HKU 7/CRF/09). I.O.L. Ng is Loke Yew Professor in Pathology.

Acknowledgement: The authors would like to thank LKS Faculty of Medicine at The University of Hong Kong for the Faculty Core Facility.

Summary

Tumor-initiating cells (T-ICs) are a subpopulation of chemoresistant tumor cells that have been shown to cause tumor recurrence upon chemotherapy. Identification of T-ICs and their related pathways are therefore priorities for the development of new therapeutic paradigms. We established chemoresistant hepatocellular carcinoma (HCC) xenograft tumors in immunocompromised mice in which an enriched T-IC population was capable of tumor initiation and self-renewal. Using this model, we found CD24 to be up-regulated in residual chemoresistant tumors when compared with bulk tumor upon cisplatin treatment. $CD24^+$ HCC cells were found to be critical for the maintenance, self-renewal, differentiation, and metastasis of tumors and to significantly impact patients' clinical outcome. Using a lentiviral-based knockdown approach, CD24 was found to be a functional liver T-IC marker that drives T-IC genesis through Stat3-mediated Nanog regulation. Our findings point to a CD24 cascade in liver T-ICs that may provide an attractive therapeutic target for HCC patients.

Introduction

Hepatocellular carcinoma (HCC) is the fifth most common cancer in the world (Jemal et al., 2008). The first line treatment for HCC is liver transplantation or surgical resection (Carr, 2004, Kassahun et al., 2006). However, most HCCs are inoperable as patients present at advanced stages. Even after surgical resection, the long-term prognosis of HCC remains unsatisfactory due to high recurrence rates. For HCC patients in advanced stages, chemotherapy via either transarterial chemoembolization or a systemic route is the second-line treatment. Unfortunately, the overall response rate is unsatisfactory due to the highly chemoresistant nature of the tumor and the toxicity of the chemotherapeutic agents (Aguayo and Patt, 2001, Llovet and Bruix, 2003, Kuvshinoff and Ota, 2002). Further investigation into the mechanism of chemoresistance of HCCs is needed to improve the survival rate.

The cancer stem cell hypothesis posits that cancers are maintained in a hierarchical organization of rare 'cancer stem cells' (or tumor-initiating cells, T-ICs), which divide rapidly into amplifying cells and differentiated tumor cells (Dalerba et al., 2007). Owing to this unique survival mechanism, this rare population of cells is resistant to the current chemotherapies (All-Hajj, 2007). This hypothesis also provides an explanation for the failure of current treatment regimes due to the fact that they are largely targeted at eradicating the rapidly proliferating tumor bulk. The existence of T-ICs was first evidenced in acute myeloid leukemia (Lapidot et al., 1994) and more recently in different solid tumors, including those of the brain (Singh et al., 2003), colon (O'Brien et al., 2007), breast (Al-Hajj et al., 2003), prostate (Collin et al., 2005), melanoma (Fang et al., 2005), and pancreas (Hermann et al., 2007). Integrative comparative genomic analysis has established molecular similarities between T-ICs and normal tissue stem cells, suggesting a role for liver T-ICs in hepatocarcinogenesis (Marquardt et al., 2010). Recently, liver T-ICs have been identified by several cell surface antigens such as CD133 (Ma et al., 2007 and 2010), CD90 (Yang et al., 2008), and EpCAM (Yamashita et al., 2009), and these T-ICs are capable of self-renewal and were found to be resistant to chemotherapeutic drugs (Ma et al., 2008).

Because T-ICs are relatively resistant to chemotherapy, we enriched for liver T-ICs by establishing chemoresistant HCC xenograft tumors in immunocompromised mice, mimicking the clinical situation under which HCC patients receive chemotherapy. Using this model, we identified CD24, a mucin-like cell surface glycoprotein, to be up-regulated in residual chemoresistant tumors upon cisplatin treatment when compared with untreated tumors. To further investigate the role of $CD24^+$ cells in HCC, we isolated these cells from the HCC cell lines PLC/PRF/5 and HLE and HCC clinical samples. Freshly isolated $CD24^+$ cells were found to be more quiescent, greater ability to form tumors in NOD/SCID mice, the ability to self-renew, differentiation and metastasis. The clinical impact of CD24 was also addressed, and it was found to significantly correlate with aggressive tumor behavior. Knockdown of CD24 by a lentiviral-based shRNA approach suppressed the stem/progenitor cell characteristics, suggesting that CD24 is a functional marker of liver T-ICs. Furthermore, we identified Nanog to be an important downstream effector of CD24-mediated HCC tumorigenicity and self-renewal. cDNA microarray analysis revealed that regulation of *Nanog* by CD24 was Stat3-dependent. Our findings may provide an attractive therapeutic approach of targeting the CD24 cascade in liver T-ICs to achieve better clinical outcomes for HCC patients.

Results

CD24 was elevated in self-renewing liver cancer cells enriched by chemotherapy in an HCC xenograft model

According to the 'cancer stem cell' hypothesis, chemotherapy reduces the tumor burden while sparing a T-IC population endowed with drug-resistant properties (Ma et al., 2008, Pardal et al., 2003). In order to determine whether liver T-ICs are enriched upon chemotherapy, a chemoresistant xenograft model derived from HCC cell lines was established that mimics the heterogeneity observed in patients' tumors. Tumor xenografts derived from PLC/PRF/5 cells were subcutaneously inoculated into nude mice. When the tumors reached 4 mm in diameter, the mice were injected intra-peritoneally with various doses of cisplatin. Such treatment resulted in variable tumor inhibition among the xenografts (Figure 1A). The dosage of cisplatin for establishment of chemoresistant tumor was determined experimentally by comparing the tumor response to several different dosages ranging from 1 mg/kg to 5 mg/kg. From the dose response curve, 5 mg/kg was chosen as the level at which further increase of cisplatin concentration did not further reduce the tumor size (Figure 1B). To verify whether cisplatin at 5 mg/kg enriched the proportion of T-ICs in the residual chemoresistant tumor, single HCC cells derived from untreated (control group) and chemoresistant residual tumors (chemoresistant group) were isolated. The tumorigenicity of the HCC cells derived from these two groups was compared after serial orthotopic transplantation of $5x10^4$ corresponding cells into SCID mice. Because the PLC/PRF/5 cells were labeled with the luciferase gene, the tumorigenicity was evaluated using a xenogen imaging system. Compared with HCC cells from untreated tumor, enhanced tumor-forming and self-renewal abilities were observed in chemoresistant residual HCC cells, indicating successful enrichment for liver T-ICs in this chemoresistant HCC xenograft model derived from PLC/PRF/5 cells (Figure 1C). To further determine what markers are elevated in self-renewing chemoresistant HCC cells, the messenger RNA profiles from tumors derived from the untreated and chemoresistant groups (5 mg/kg) were compared using a cDNA microarray containing 34,000 genes (data not shown, unpublished). CD24,

but not other currently known liver T-IC markers (CD133, CD90, and EpCAM), was found to be up-regulated by two folds in the chemoresistant group compared to the control group. To validate this observation, we studied the expression of *CD24* by qPCR and immunohistochemistry (IHC) in the tumors. Consistent with the cDNA microarray data, *CD24* was found to be up-regulated by three folds by qPCR (Figure 1D). Similarly, IHC studies also showed that CD24 expression was dramatically higher in the chemoresistant group relative to the control group (Figure 1E). To exclude the possibility of a cell-type specific effect, CD24 expression was further evaluated in the same chemoresistant model using another HCC cell line, Huh-7. By IHC staining, CD24 expression was dramatically higher in the chemoresistant group (Figure S1).

CD24 expression in HCC cell lines and human HCC sspecimens

To determine whether CD24 marks more tumorigenic liver cells, we examined its expression by flow cytometry (FACS) analysis in a panel of liver cell lines, including the non-tumorigenic immortalized cell line MIHA and the HCC cell lines Huh-7, Hep3B, BEL7402, PLC/PRF/5, HLE, BEL7402, MHCC-97L, MHCC-97H, and MHCC-LM3. Variable expression of CD24 was found in the HCC cell lines with *in vivo* tumor forming ability. In contrast, the immortalized non-tumorigenic cell line MIHA, which is incapable of tumor formation *in vivo* showed no CD24 expression (Figure 1F). These results suggest that CD24 expression might play a role in tumor development *in vivo*. Next, we asked whether CD24 was overexpressed in patient HCC specimens when compared with non-tumor counterparts. We performed IHC staining for CD24 on 41 human HCC tissue samples as well as their non-tumor counterparts. The percentage of $CD24^+$ cells in the HCC specimens ranged from 0% to 16%, whereas there was no CD24 expression in the non-tumor counterparts. Among all HCC specimens, over 70% (29/41) of the cases showed CD24 expression in less than 2% of cells (Figure 1G & 1H). Thus, CD24 was expressed sporadically in human HCC specimens.

$CD24^+$ HCC cells possessed characteristics of stem/progenitor cells

T-ICs are believed to possess the stem/progenitor properties of relative quiescence (Friel et al., 2008), self-renewal (Patrawala et al., 2005), and tumorigenicity in immunodeficient mice (Li et al., 2007). First, we determined whether $CD24^+$ HCC cells were more tumorigenic than their $CD24^-$ counterparts *in vivo* by tumor-forming assay using $CD24^+$ and $CD24^-$ cells purified from PLC/PRF/5 and HLE cell lines. Purified cells were inoculated subcutaneously into NOD/SCID mice. A significant difference in tumor incidence was observed between $CD24^+$ and $CD24^-$ cells (Figure 2A & 2B). As few as 500 $CD24^+$ cells were sufficient for consistent tumor development in NOD/SCID mice (Table S1A & 1B). A key property of stem cells, including T-ICs, is their unique ability to undergo self-renewal (Patrawala et al., 2005). One method of evaluating self-renewal capacity is by testing serial passage ability. After xenografts derived from sorted PLC/PRF/5 cells formed, the corresponding tumors were excised from the primary recipients, dissociated into a single-cell suspension, grown in culture for approximately one week, re-sorted into $CD24^+$ and $CD24^-$ cells using an antibody specific to human CD24, and then re-injected into secondary mouse recipients. About three weeks, all the secondarily xenografted mice injected with $CD24^+$ cells showed tumor formation that reconstituted the phenotypic heterogeneity of the primary xenografts (Figure 2A & 2B), providing direct evidence of the self-renewal ability of the cell population. Consistently, as few as 500 $CD24^+$ cells were sufficient for tumor formation (Table S1C). In addition, all secondary xenografts formed around three weeks, a significantly shorter tumor latency period than for the primary xenografts. Normal and neoplastic stem-like cells from epithelial organs can be expanded as sphere-like aggregates in serum-free EGF-bFGF-supplemented medium and undergo serial passage (Liu et al., 2005). To obtain further evidence for the self-renewal ability of $CD24^+$ cells, we performed a sphere formation assay. Compared with $CD24^-$ cells, significantly larger and more hepatospheres were observed in $CD24^+$ cells isolated from both PLC/PRF/5 and HLE cells (Figure 2C), which supports the greater self-renewal capability of $CD24^+$ HCC cells. It is believed that quiescence is one of the characteristics of stem cells (Friel et al., 2008). To compare

the relative quiescence of $CD24^+$ and $CD24^-$ cell fractions, cell proliferation rate was measured. Colony formation assay revealed that $CD24^+$ cells derived from PLC/PRF/5 and HLE proliferated at a significantly lower rate than $CD24^-$ cells (P <0.010 and P <0.001, respectively, t test, Figure 2D). Finally, we addressed whether $CD24^+$ cells had other intrinsic properties of stem cells by examining the expression of certain 'stemness' associated genes that are crucial in pathways and programs that establish and maintain stem cell-like characteristics. Using qPCR analysis, we found that $CD24^+$ fractions purified from both PLC/PRF/5 and HLE cells had a general overexpression of these genes (Figure 2E).

Clinical ssignificance of CD24 in HCC

We have demonstrated that sorted $CD24^+$ cells derived from HCC cell lines possess stem/progenitor characteristics (Figure 2). To examine the role of $CD24^+$ HCC cells in HCC patients, we isolated single HCC cells from fresh HCC clinical samples and separated them into $CD24^+$ and $CD24^-$ cell populations. We examined whether $CD24^+$ HCC cells derived from HCC clinical samples also possessed tumorigenicity and self-renewal ability. In colony formation assays, $CD24^+$ HCC cells were able to induce more and larger tumor colonies than their $CD24^-$ counterparts (P<0.001, t test) (Figure 3A) and this showed that $CD24^+$ HCC cells were more tumorigenic than $CD24^-$ cells *in vitro*. To evaluate the *in vivo* tumorigenicity, two fresh HCC patient samples were used. By flow cytometry, corresponding $CD24^+$ and $CD24^-$ cells were sorted from patient #71 and patient #73, and their CD24 expression was found to be 15% and 2%, respectively. As few as 4,000 $CD24^+$ HCC cells are able to develop a tumor in NOD/SCID mice, while there was no tumor formation with $CD24^-$ cells after 70 days of tumor inoculation (Figure 3B & 3C). The capacity of $CD24^+$ cells for self-renewal was also evidenced by sphere formation assays and evaluation of stemness genes by quantitative PCR. $CD24^+$ HCC cells preferentially expressed stemness genes and were able to survive in anchorage-independent serum-free EFG-FGF supplemented medium (Figure 3D & 3E). CD24 expression was previously found to be

overexpressed in HCC and has prognostic significance (Huang and Hsu, 1995; Yang et al., 2009). Next, we investigated the potential relationship between CD24 expression and the clinical outcome of HCC patients. We retrospectively analyzed the *CD24* expression in 46 HCC patients by quantitative PCR. The cut off value of T/N >3 was used to determine *CD24* expression in HCC patients. Eighteen (39.1%) of the 46 cases showed more than three-fold *CD24* overexpression in the HCC tumor tissues as compared with the corresponding non-tumorous liver tissues, and these were considered the high CD24 expression group. The correlation between *CD24* overexpression and the clinico-pathologic features is summarized in Table 1. Patients whose tumors had high *CD24* expression had a significantly higher risk of tumor recurrence in the first year after surgery (P=0.002, χ^2 test), and higher serum AFP level (P=0.009, χ^2 test). Their tumors more frequently had venous infiltration (P=0.003, χ^2 test), presented at advanced tumor stages (P=0.010, χ^2 test). Patients with *CD24* overexpression in their tumors had significantly shorter disease-free survival than those with low CD24 expression (P=0.002, log-rank test) (Figure 3F). Consistently, patients with *CD24* overexpression had shorter overall survival, though this did not reach statistical significance (P=0.113, log-rank test) (Figure 3F). All in all, *CD24* overexpression in HCC correlated with more aggressive tumor behavior and worse clinical outcome.

$CD24^+$ HCC cells had the capacity to metastasize *in vivo*

Venous infiltration is an important pathologic feature determining HCC metastasis and tumor recurrence (Arii et al., 1992). As shown in Table 1, high *CD24* expression significantly correlated with venous infiltration. This finding suggests that $CD24^+$ cells are endowed with metastatic features. To test this hypothesis, we first isolated $CD24^+$ and $CD24^-$ cells from PLC/PRF/5 and examined their invasive and migratory abilities using matrigel invasion and transwell migration assay, respectively. Prior to each experiment, trypan blue assay was performed to show that cell viability of sorted cells from both subpopulations was greater than 90% (data not shown). As compared to $CD24^-$ cells, $CD24^+$ cells displayed approximately 3.7-fold and 5-fold higher cell

migration and invasion efficiency, respectively ($P<0.001$, *t* test) (Figure 4A & 4B). To test the *in vivo* metastatic role of $CD24^+$ cells, an experimental metastasis model was employed in which $1x10^5$ $CD24^+$ or $CD24^-$ cells were injected into NOD/SCID mice through tail vein injection. After 40 days, the formation of tumor foci in the lungs was evaluated with a xenogen imaging system. Three out of five (60%) mice injected with $CD24^+$ cells showed tumor formation in the lungs, whereas none of the mice injected with $CD24^-$ cells showed tumor formation in the lungs (Figure 4C & 4D). In addition, lung metastasis was also observed in NOD/SCID mice after subcutaneous injection of $CD24^+$ derived from patient #71 and #73 (Figure S2A). Histological evidence for the lack of tumorigenicity in NOD/SCID mice inoculated with $CD24^-$ cells is shown in Figure S2B. These data support the hypothesis that $CD24^+$ T-ICs represent a distinct invasive T-IC population that contributes to tumor metastasis. Recent studies have suggested that CD133 and EpCAM are putative T-IC markers for HCC (Ma et al., 2007, Yamashita et al., 2007). By flow cytometric analysis, we examined and compared the expression of each marker in Huh-7 cells. CD24 expression was found to overlap with that of CD133 and EpCAM, suggesting that these three markers share similar self-renewal pathways (Figure S3A). Contrary to CD133 and EpCAM, we observed only a very low, if at all, overlapping expression between CD24 and CD90 (~1%) (data not shown). In view of this, we proceeded to examine whether CD24 serves a unique function of liver T-IC over CD90 using a CD90 lentiviral based shRNA knockdown approach in MHCC97H cells, which was found to contain the highest CD24 expression among a panel of liver cell lines tested (Yang et al., 2008). CD90-repressed clones (shRNA CD90) or CD90 expressing clones (non-target control) were first sorted for $CD24^+$ and $CD24^-$ cells; and then examined for differential tumorigenic capacity (Figure S3B). $CD24^+$ liver T-ICs were found to be more tumorigenic than $CD24^-$ non-T-ICs. Further, the ability of $CD24^+$ CD90 expressing or knockdown cells to initiate tumor formation were very similar, with a tumor initiation rate of 83.3% and 75%, respectively (Figure S3C). Thus, we concluded that CD24 do serve as a unique function in the T-ICs of HCC.

CD24$^+$ HCC cells had the capacity to differentiate *in vitro*

To investigate the differentiation capacity of CD24$^+$ cells, we first cultivated the cells dissociated from fresh HCC clinical tissues in such specified medium as 'hepatospheres', to obtain undifferentiated cells. These hepatospheres were serially passaged by trypsinization into single cells to re-form new hepatospheres and, after three passages, all the floating hepatospheres were observed to be CD24$^+$ (data not shown), suggesting the inability of CD24$^-$ cells to survive in serum-free conditions. To evaluate the differentiation potential of CD24$^+$ cells, hepatospheres were cultivated without EGF or FGF in the presence of 10% serum. After one day of culture, floating undifferentiated cells attached to the glass, gradually flattened out from the hepatospheres, and became large and adherent cells. Upon differentiation, the hepatospheres gained CK18 expression and lost CD24 expression, and they acquired a morphology closely resembling the HCC cells present in the original tumor (Figure 4E). By qPCR, we found consistent decline in CD24 and 'stemness'-associated genes upon differentiation of the hepatospheres derived from HCC patient samples (Figure 4F). The same phenomenon was observed upon differentiation of the hepatospheres derived from the HCC cell line PLC/PRF/5 (Figure 4G). To further explore the capacity of CD24$^+$ cells to differentiate, highly purified CD24$^+$ and CD24$^-$ cells were separately cultured in 10% serum-supplemented medium for two weeks, following which the expression of CD24 was analysed in each population by flow cytometry. We found that the CD24$^+$ proportion dramatically declined after three days, and reverted almost to the pre-sorting level, whereas CD24$^-$ cells retained low expression of CD24 even after two weeks, indicating that CD24$^-$ cells arose only from CD24$^+$ cells and not *vice versa* (Figure 4H). In addition, by single cell sorting, increase in CK18 expression was observed in CD24$^+$ cells but not in CD24$^-$ cells upon differentiation (Figure S4).

CD24 knockdown reduced stem/progenitor characteristics in HCC cells

It is yet to be proven whether T-IC cell surface markers are just physical markers or whether they

functionally contribute to the traits of stem/progenitor cells. Therefore, we performed a CD24 knockdown experiment using a lentiviral-based approach in cells that highly express CD24 (Huh-7 and PLC/PRF/5). After confirmation of successful knockdown with a 50% to 60% reduction (Figure 5A & 5B) in CD24 expression in clones #121 and #278, respectively, in both Huh-7 and PLC/PRF/5, we first compared the expression of 'stemness'-associated genes between CD24 knockdown clones and non-target controls. Compared with the non-target controls, these genes, including *Sox2*, *Oct4*, and *Nanog*, were down-regulated in Huh-7 and PLC/PRF/5 knockdown clones (#278) (Figure 5A & 5B). Consistent down-regulation of the above stemness genes was observed in clone #121 (data not shown). Next, we examined the tumorigenicity of Huh-7 cells upon CD24 knockdown. After four weeks, we found that both the number and size of the tumors was lower in clone #278 when compared with the non-target control group (Figure 5C & Table S2). The effect of CD24 knockdown on tumorigenicity was also examined in PLC/PRF/5 cells. Either CD24 knockdown cells or control cells (15,000) were injected into the liver of SCID mice. The incidence of tumor formation was 60% (3/5) whereas it was 20% (1/5) in the CD24 knockdown group (Figure 5D). In the control group, all SCID mice showing tumor formation exhibited lung metastasis. However, no lung metastasis was observed in the CD24 knockdown group, further suggesting the metastatic role of CD24 in HCC (Figure 5E). The effect of CD24 knockdown on cell proliferation was also examined with the colony formation assay. We found that CD24 knockdown cells proliferated more rapidly than the non-target control cells (Figure 5F). The effect of CD24 knockdown on self-renewal was also examined by sphere formation assay. We found that CD24 knockdown cells generated fewer and smaller hepatospheres in their first and second passages (Figure 5G). In addition, knockdown of CD24 in Huh-7 cells increased the sensitivity of cells to both cisplatin and doxorubicin (Figure S5A). Similarly, by cell sorting approach, $CD24^+$ HCC cells derived from PLC/PRF/5 were more chemoresistant than $CD24^-$ cells (Figure S5B).

CD24 drove tumor initiation and self-renewal by mediating a self-renewal gene, *nanog*

To determine the major downstream mediator of CD24 in tumor initiation and self-renewal, we scrutinized the qPCR data for effects of CD24 on 'stemness'-associated genes by both cell sorting and lentiviral-knockdown approach. The effect of CD24 on the expression of 'stemness'-associated genes in both HCC cell lines and clinical samples is summarized in Table S3. Among the genes we examined, *Nanog* and *Sox2* were found to be consistently altered upon loss of CD24 in the four HCC cell lines and two HCC clinical samples studied. To further identify the major mediator of CD24 function, we sought a correlation between the expression of CD24 with *Nanog* and *Sox2* in five HCC cell lines that expressed different levels of CD24. In these five HCC cell lines, CD24 expression positively correlated with *Nanog* expression but not with *Sox2* (Figure 6A & S6A). Next, we examined the correlation between *CD24* and *Nanog* by qPCR using the same cohort of HCC patients. Consistently, *CD24* significantly correlated with *Nanog* expression in these 46 HCC patient samples (P=0.026; r=0.325, Pearson's correlation) (Table S4, Figure 6B). To determine whether CD24 drives tumor initiation and self-renewal by activating *Nanog* gene expression, we overexpressed *Nanog* in a CD24 knockdown clone (#278) of Huh-7 cells to investigate whether the effect of CD24 knockdown could be eliminated upon transfection with *Nanog*. Using the lentiviral approach, *Nanog* was overexpressed in a CD24 knockdown clone (#278) of Huh-7 cells and the expression level was comparable to the non-target control (Figure 6C). After successful confirmation of *Nanog* overexpression in the CD24 knockdown Huh-7 cells, we compared in SCID mice the tumor forming abilities of CD24 knockdown Huh-7 cells with and without *Nanog* overexpression. The tumorigenicity of CD24 knockdown cells increased upon *Nanog* transfection, and it was comparable to that of the non-target controls (Figure 6D, Table S5). The effect of *Nanog* overexpression on the self-renewal ability of CD24 knockdown Huh-7 cells was also studied using the sphere formation assay. This revealed that CD24 knockdown cells generated greater and larger hepatospheres in their first and second passages upon *Nanog* overexpression (Figure 6E). This result provides direct evidence that CD24 mediates tumor initiation and self-renewal by driving up *Nanog* expression.

CD24 regulated *nanog* expression through Stat3 phosphorylation

Being a transmembrane protein (Sammar et al., 1997), CD24 should be able to transmit extracellular signals to the nucleus to activate *Nanog* expression. In order to identify the cytoplasmic mediator linking CD24 and Nanog, a cDNA microarray (the Affymetrix Human genome U133 gene chip) was used to compare the gene expression profiles of CD24 knockdown Huh-7 cells and non-target control cells. By Ingenuity Pathway analysis, several canonical pathways were identified, among which 'acute phase response signaling' was found to be the most significantly altered (Figure S6B). One of the key components of this signaling cascade is the IL6 pathway, a pathway important for liver stem cell maintenance, in which phosphorylation of Stat3 at the Tyrosine705 residue is critical (Lin et al., 2009, Tang et al., 2008). The pathway analysis suggested the importance of Stat3 phosphorylation in the IL6 pathway, as the expression of several genes downstream of Stat3 was altered upon CD24 knockdown (Figure S6C). In embryonic stem cells, phosphorylated Stat3 was found to bind to the murine *Nanog* promoter and activate its transcription (Suzuki et al., 2006). We therefore hypothesized that CD24 transcriptionally regulated *Nanog* expression through Stat3 phosphorylation. To test this hypothesis, we first examined the expression of Stat3 and its phosphorylated form in CD24 knockdown clones of Huh-7 and PLC/PRF/5 cells. We found less phosphorylated Stat3 (Y705) upon CD24 knockdown but not so for its parental form (Figure 6F); this is consistent with the cDNA microarray finding that there was no change in the mRNA level of Stat3. To further examine whether the regulation of *Nanog* expression in HCC cells is Stat3 dependent, we examined pStat3 (Y705) and Nanog expression in response to a Stat3 inhibitor (S3I-201) in PLC/PRF/5 and Huh-7 cells. Nanog expression was found to be down-regulated upon S3I-201 treatment in a dose-dependent manner (Figure S7A). This observation was further confirmed when we found overexpression of CD24 ORF into CD24 negative cells, MIHA, resulted in a significant increase in pStat3 (Y705) and Nanog expression; while addition of varying doses of S3I-201 led to abolishment of this effect (Figure S7B). To validate the transcriptional regulation of *Nanog* by CD24, we transfected a GFP-tagged *Nanog*

promoter into PLC/PRF/5 cells to monitor its activity. By FACS-sorting, the GFP signal was found to be notably higher in the $CD24^+$ fraction, reflecting up-regulation of *Nanog* transcription, and this signal was decreased upon addition of S3I-201 (Figure 6G). To further examine the potential binding between phosphorylated Stat3 and the Nanog promoter, a ChIP-qPCR assay was performed. In Figure 6H, we demonstrated binding between phosphorylated Stat3 and Nanog promoters in Huh-7 and PLC/PRF/5 cells. Conversely, upon CD24 knockdown, there was a decrease of p-Stat3 binding on the Nanog promoters in these two cell lines. CD24 was previously found to be associated with Src-associated kinase (Sammar et al., 1997), which phosphorylates Stat3 (Byers et al., 2009). By overexpression and knockdown approaches, activated form of Src (pY416) was consistently altered but not JAK2, another molecule that has previously been found to phosphorylate Stat3 (Hedvat et al., 2009) (Figure S7C-E), which suggests that CD24 potentially phosphorylates Stat3 through Src but not JAK. These findings demonstrate the positive link between CD24 expression, STAT3 activation and *Nanog* transcription.

Discussion

According to the 'cancer stem cell hypothesis', T-IC populations become enriched upon chemotherapy due to their unique survival mechanism. Recently, this theory has been experimentally proven in various cancer systems including breast and lung cancer (Bertolini et al., 2009, Yu et al., 2007). In this study, we successfully enriched for liver T-ICs using a chemoresistant HCC xenograft model. In this model, cisplatin-treated HCC cells showed enhanced self-renewal capacity and tumorigenicity when compared with untreated control cells. By cDNA microarray, we found that CD24 was up-regulated in the enriched T-IC population, and this was confirmed by qPCR and IHC staining. To eliminate the possibility that up-regulation of CD24 upon chemotherapy was a cell-type specific effect, we confirmed CD24 up-regulation by IHC staining using xenografts derived from another HCC cell line, Huh-7.

The *CD24* gene encodes a heavily glycosylated cell surface protein anchored to the membrane by phosphatidylinositol (Pirruccello et al., 1986). *CD24* is an oncogene, which are overexpressed in various human malignancies (Kristiansen et al., 2002, Kristiansen et al., 2003). It also plays a role during the embryonal development of pancreatic cells (Cram et al., 1999). Recent studies have suggested that CD24 may be a negative T-IC marker with specific regards to breast cancer (Al-Hajj et al., 2003). Intriguingly, increasing evidence has shown that $CD24^+$ tumor cells are T-ICs for gastrointestinal cancers such as colon cancer (Yeung et al., 2010), pancreatic cancer (Li et al., 2007), and cholangiocarcinoma (Wang et al., 2010). To determine whether $CD24^+$ cells were liver T-ICs, we isolated $CD24^+$ and $CD24^-$ fractions from HCC cell lines and human HCC samples by cell sorting. We found that $CD24^+$ HCC cells showed higher tumorigenicity than their $CD24^-$ counterparts in NOD/SCID mice. In addition, $CD24^+$ HCC cells were capable of self-renewal, as they could propagate in another mouse recipient upon serial transplantation. The self-renewal ability of $CD24^+$ HCC cells was further evidenced by the more and larger hepatospheres they generated in sphere formation assays when compared with their $CD24^-$ counterpart. The above phenotype was also associated with increased expression of stemness genes. Consistently, $CD24^+$

HCC cells were found to be more quiescent and to proliferate more slowly in colony formation assays. Moreover, $CD24^+$ HCC cells were able to differentiate into $CD24^-$ cells, but not *vice versa* by single cell sorting approach.

To examine whether CD24 was specific for liver T-ICs, we performed CD24 immunostaining of 41 paraffin-embedded HCC clinical samples and their non-tumor counterparts. We found that only a minority of HCC cells showed CD24 expression, whereas no CD24 expression was observed in the non-tumor liver tissues. Flow cytometric analysis also suggested scanty expression of CD24 in several fresh HCC clinical samples (data not shown). Using qPCR on HCC resected specimens; we found that *CD24* overexpression was significantly associated with shorter disease-free survival of patients. In addition, CD24 overexpression was significantly correlated with early recurrence of HCC after surgery in the present study, suggesting the ability of $CD24^+$ tumor cells to re-establish tumor growth. These data support a previous study showing that CD24 is a useful predictive marker for early recurrence of HBV-related HCC (Woo et al., 2008). It has been predicted that T-ICs might also primarily be responsible for the formation of tumor metastases (Dalerba and Clarke, 2007). CD24 overexpression was also significantly correlated with venous infiltration, which is an important clinico-pathologic feature of HCC metastasis. Both *in vitro* and *in vivo* data demonstrate that $CD24^+$ HCC cells alone have the capacity to initiate and sustain tumor growth, leading eventually to cancer metastasis. Thus far, CD133 and EpCAM have been identified as putative T-IC markers for HCC (Ma et al., 2007, Yamashita et al., 2009). However, their metastatic potential has not been investigated. Using flow cytometric analysis, we found that CD24 expression overlapped with the expression of both CD133 (~90.9%) and EpCAM (~55.8%), suggesting that they may share common self-renewal pathways. However, unlike CD24, $CD133^+$ liver T-ICs have previously been found to have a greater proliferative potential than $CD133^-$ counterparts (Ma et al., 2007). We do not, at the moment, have an explanation to why CD24 and CD133 subpopulations display different proliferative potential, as demonstrated by colony formation assay. Yet, we speculate that since CD24 expression do not completely overlap

with CD133 (9.1% $CD24^+CD133^-$) and EpCAM (44.2% $CD24^+EpCAM^-$), it is possible that these T-IC markers may display different tumorigenic and metastatic potentials. In terms of their tumorigenic potential, $2x10^4$ $CD133^+$ and $1x10^4$ $EpCAM^+$ HCC cells derived from patient samples were previously reported to be needed for efficient tumor formation in immunodeficient mice (Ma et al., 2010; Yamashita et al., 2009). And in our current study, we found that as few as 4,000 $CD24^+$ HCC cells were sufficient for consistent tumor initiation.

Unlike CD133 and EpCAM, CD24 showed only very low overlapping expression with CD90. Using a CD90 shRNA knockdown approach, CD90-repressed clones or CD90 expressing clones were sorted for $CD24^+$ and $CD24^-$ cells. The tumorigenicity of $CD24^+$ CD90 expressing or knockdown cells were found to be very similar indicating that CD24 can serve as a unique function in the T-ICs of HCC. In terms of metastatic potential, 5,000 $CD90^+$ liver T-ICs was previously reported to induce lung metastasis following orthotropic injection in 50% of the animals examined (Yang et al., 2008) while in our current study, we found that only 4,000 $CD24^+$ liver T-ICs derived from patient samples was sufficient to induce lung metastasis following subcutaneous injection in 100% of the animals tested. These results demonstrate the superiority of CD24 in some aspects over currently available liver T-IC markers.

Using lentiviral-based RNA interference approach, CD24 was found to be functional liver T-IC marker. Also, in an orthotopic HCC tumor model, CD24 knockdown not only inhibited the growth of tumors but also inhibited metastasis to the lungs of SCID mice. Furthermore, we found that stemness genes such as *Oct4, Sox2,* and *Nanog* were down-regulated when CD24 was knocked down, suggesting a crosstalk between CD24 signaling and stemness gene expression. Interestingly, we found a significant correlation between CD24 expression and *Nanog* expression in a panel of HCC cell lines and HCC clinical samples. *Nanog* is a self-renewal gene that maintains the pluripotency of embryonic stem cells (Silva et al., 2009). Recently, *Nanog* was identified as a new oncogene by large-scale oncogenomic analysis (Mattison et al., 2010), and *Nanog* expression regulates human tumor development (Jeter et al., 2009). To determine if CD24 drove tumor

initiation and self-renewal through activation of *Nanog* gene expression, we overexpressed *Nanog* in a CD24 knockdown clone (#278) of Huh-7 cells. We found that the effect of CD24 knockdown was eliminated upon transfection of *Nanog*, demonstrating that CD24 up-regulates *Nanog* expression to initiate tumor formation and self-renewal. However, by western blot analysis, we found that CD24 expression did not change upon overexpression of *Nanog* and inhibition of Stat3 (data not shown). This indicates that Nanog and Stat3 truly are downstream targets of CD24.

By cDNA microarray comparison of gene expression between CD24 knockdown cells and control cells, we found that the IL6/Stat3 pathway was significantly down-regulated upon CD24 knockdown. The IL6/Stat3 pathway has been previously demonstrated to play important roles in the maintenance and proliferation of liver T-ICs (Lin et al., 2009, Tang et al., 2008). CD24 is associated with Src-associated kinase (Sammar et al., 1997), which phosphorylates Stat3 (Byers et al., 2009). By overexpression and shRNA knockdown approaches, pY416-Src was consistently altered with phosphorylated Stat3 (Y705) and Nanog expression, which suggests that CD24 might act on Stat3 through Src. By ChIP assay, we found binding of phosphorylated Stat3 (Y705) to Nanog promoter, which is consistent to the previous study shown in murine system (Suzuki et al., 2006). Upon CD24 knockdown in Huh-7 and PLC/PRF/5, there was reduced binding between phosphorylated Stat3 (Y705) and Nanog promoter. By western blot analysis, we found that less phosphorylated Stat3 (Y705) was observed in CD24 knockdown cells. It is controversial whether *Nanog* is regulated in a Stat3-dependent manner (Humphrey et al., 2004). Nanog expression was found to be reduced in a dose-dependent manner upon addition of S3I-201, indicating a regulatory role of Stat3 on Nanog expression. Using GFP as a reporter of *Nanog* promoter activity, we found that $CD24^+$ PLC cells showed higher *Nanog* promoter activity, and this activity was reduced upon addition of S3I-201. This result suggests that CD24 activates *Nanog* promoter in a Stat3-dependent manner.

Current chemotherapy against HCC usually primarily directs against the bulk population of the tumor. Although these therapies are able to initially shrink the primary tumors, they fail to

consistently eradicate the lesions, leading to tumor relapse. In this study, we identified $CD24^+$ HCC cells within these small lesions, and they functioned to initiate tumor growth and self-renewal through Stat3-mediated Nanog up-regulation. The identification of CD24 signaling pathways provides an attractive therapeutic strategy against this deadly disease.

Experimental Procedures

Human HCC tissue collection and processing. Liver tumor and adjacent non-tumor liver tissue specimens were collected from six patients (Patient #3, 36, 38, 51, 71, and 73) (age ranging from 37 to 82) who underwent hepatectomy for HCC between 2008 and 2010 in the Department of Surgery, Queen Mary Hospital, Hong Kong, with Institutional Review Board (IRB) approval. Tumor tissue from xenografts and fresh tumors was minced into 1 mm^3 cubes and incubated with Type IV Collagenase (Sigma, St. Louis, MO) for 5-10 minutes at 37°C. A single-cell suspension was obtained by filtering the supernatant through a 100-μm cell strainer (BD Biosciences, San Jose, CA). Cell viability was assessed by trypan blue exclusion staining and counting using a hemocytometer. For fresh clinical tumors, removal of $CD45^+$ cells from within the tumor was done with a CD45 depletion kit (Miltenyi Biotech, Germany).

Isolation of $CD24^+$ and $CD24^-$ populations by flow cytometry and magnetic bead cell sorting. For magnetic cell sorting, cells were labeled with PE-conjugated CD24 antibody (clone ML5) (BD Pharmingen, San Jose, CA) followed by anti-PE microbeads (Miltenyi Biotec, Germany). Sorting was carried out using the Miltenyi Biotec MACS Cell Separation Kit according to the manufacturer's instructions. Magnetic separation was performed up to three times to obtain a $CD24^+$ population more than 95% pure. Aliquots of $CD24^+$ and $CD24^-$ sorted cells were evaluated for purity with a FACSCalibur machine and CellQuest software (BD Biosciences San Jose, CA). For isolation of $CD24^+$ and $CD24^-$ cell populations, cells were stained with PE-conjugated CD24 antibody (BD Biosciences, San Jose, CA) and with isotype-matched mouse immunoglobulin as a control. Samples were analyzed and sorted on a BD FACSAria (BD Biosciences San Jose, CA). For the positive and negative populations, only the top 10% most brightly stained cells and the bottom 10% most dimly stained cells were selected, respectively. Aliquots of $CD24^+$ and $CD24^-$ sorted cells were evaluated for purity with a FACSCalibur machine and CellQuest software (BD Biosciences San Jose, CA).

In Vivo tumorigenicity experiments. Different numbers of cells were injected subcutaneously either into severe combined immunodeficient (SCID)-beige or non-obese diabetic (NOD)/SCID mice. For an orthotopic tumor model, approximately 15,000 PLC/PRF/5 cells in 30 μL of culture medium were injected into the left liver lobe of the SCID-beige mice using a method described previously (Fu et al., 1991). For those HCC cells labeled with luciferase, imaging was performed using a Xenogen IVIS 100 cooled CCD camera (Xenogen, California) on Day 40. The mice were given intraperitoneal injections with 200 μL of 15 mg/mL D-luciferin 15 min before imaging. For imaging, the mice were placed in a light-tight chamber, the acquisition time ranged from 3 sec to 1 min, and pseudoimages of the emitted light in photons/s/cm^2/steradian superimposed over the gray-scale photographs of the animal were taken.

Chemoresistant tumor model. Subcutaneous xenografts were established using the PLC/PRF/5 and Huh-7 HCC cell line. The animals used to test the treatment were 4- to 6-week-old male athymic nude mice (BALB/c-*nu/nu*). Treatment was started once the size of the xenograft reached approximately 4 mm in diameter. The mice were randomly assigned into four groups, each consisting of three mice. They were treated with cisplatin intra-peritoneally every 4 days for 4 weeks at either 1) cisplatin (1 mg/kg), 2) cisplatin (2 mg/kg) or 3) cisplatin (5 mg/kg).

Statistical analyses. All statistical analyses were performed using the statistical software SPSS 17 for Windows (SPSS Inc., Chicago, IL). Fisher's exact test was used to assess the correlation between clinico-pathological parameters and CD24 overexpression for HCC patients. Student's *t* or Mann-Whitney test was used for continuous data wherever appropriate. The survival curves were assessed by the Kaplan-Meier method, and the statistical difference between two groups was evaluated by log rank test. *P* values less than 0.05 were considered statistically significant.

References

Aguayo, A., and Patt, Y.Z. (2001). Nonsurgical treatment of hepatocellular carcinoma. Semin. Oncol. *28*, 503–513.

Al-Hajj, M. (2007). Cancer stem cells and oncology therapeutics. Curr. Opin. Oncol. *19*, 61–64.

Al-Hajj, M., Wicha, M.S., Benito-Hernandez, A., Morrison, S.J., and Clarke, M.F. (2003). Prospective identification of tumorigenic breast cancer cells. Proc. Natl. Acad. Sci. USA *100*, 3983–3988.

Arii, S., Tanaka, J., Yamazoe, Y., Minematsu, S., Morino, T., Fujita, K., Maetani, S., and Tobe, T. (1992). Predictive factors for intrahepatic recurrence of hepatocellular carcinoma after partial hepatectomy. Cancer *69*, 913-919.

Bertolini, G., Roz, L., Perego, P., Tortoreto, M., Fontanella, E., Gatti, L., Pratesi, G., Fabbri, A., Andriani, F., and Tinelli, S., et al. (2009). Highly tumorigenic lung Cancer CD133+ cells display stem-like features and are spared by cisplatin treatment. Proc. Natl. Acad. Sci. USA *106*, 16281-16286.

Byers, L.A., Sen, B., Saigai, B., Diao, L., Wang, J., Nanjundan, M., Cascone, T., Mills, G.B., Heymach, J.V., and Johnson, F.M. (2009). Recipocal regulation of c-Src and Stat3 in non-small cell lung cancer. Clin. Cancer Res. *15*, 6852-6861.

Carr, B.I. (2004). Hepatocellular carcinoma: current management and future trends. Gastroenterology *127*, 218–224.

Collin, A.T., Berry, P.A., Hyde, C., Stower, M.J., and Maitland, N.J. (2005). Prospective identification of tumorigenic prostate cancer stem cells. Cancer Res. *65*, 10946–10951.

Cram, D.S., Mclntosh, A., Oxbrow, L., Johnston, A.M., and Deaizpurua, H.J. (1999). Differenital mRNA display analysis of two related but functionally distinct rat insulinoma (RIN) cell lines: identification of CD24 and its expression in the developing pancreas. Differentiation *64*, 237-246.

Dalerba, P., Cho, R.W., and Clarke, M.F. (2007). Cancer stem cells: models and concepts. Annu. Rev. Med. *58*, 267–284.

Dalerba, P., and Clarke, M.F. (2007). Cancer stem cells and tumor metastasis: first steps into uncharted territory. Cell Stem Cell *1*, 241-242.

Fang, D., Nguyen, T.K., Leishear, K., Finko, R., Kulp, A.N., Hotz, S., Van Belle, P.A., Xu, X., Elder, D.E., and Herlyn, M. (2005). A tumorigenic subpopulation with stem cell properties in melanomas. Cancer Res. *65*, 9328–9337.

Friel, A.M., Sergent, P.A., Patnaude, C., Szotek, P.P., Oliva, E., Scadden, D.T. Seiden, M.V., Foster, R., and Rueda, B.R. (2008). Functional analyses of the cancer stem cell-like properties of human endometrial tumor initiating cells. Cell Cycle *7*, 242–249.

Fu, X., Besterman, J.M., Monosov, A., and Hoffman, R.M. (1991). Models of human metastatic colon cancer in nude mice orthotopically constructed by using histologically intact patient specimens. Proc. Natl. Acad. Sci. USA *88*, 9345–9349.

Hedvat, M., Huszar, D., Herrmann, A., Gozqit, J.M., Schroeder, A., Sheephy, A., Buettner, R., Proia, D., Kowolik, C.M., and Xin, H. et al. (2009). The JAK2 inhibitor AZD1480 potently bock Stat3 signaling and oncogenesis in solid tumors. Cancer Cell *16*, 487-497.

Hermann, P.C., Huber, S.L., Herrler, T., Aicher, A., Ellwart, J.W., Guba, M., Bruns, C.J., and Heeschen, C. (2007). Distinct populations of cancer stem cells determine tumor growth and metastatic activity in human pancreatic cancer. Cell Stem Cell *1*, 313–323.

Huang, L.R., and Hsu, H.C. (1995). Cloning and expression of CD24 gene in human hepatocellular carcinoma: a potential early tumor marker gene correlates with p53 mutation and tumor differentiation. Cancer Res. *55*; 4717-4721.

Humphrey, R.K., Beattie, G.M., Lopez, A.D., Bucay, N., King, C.C., Firpo, M.T., Rose-John, S., and Hayek, A. (2004). Maintenance of pluripotency in human embryonic stem cells is STAT3 independent. Stem Cells *22*, 522-530.

Jemal, A., Siegel, R., Ward, E., Hao, Y., Xu, Y., Murray, T., and Thun, M.J. (2008). Cancer statistics. CA. Cancer J. Clin. *58*, 71–96.

Jeter, C.R., Badeaux, M., Choy, G., Chandra, D., Patrawala, L., Liu, C., Calhoun-Davis, T., Zaehres, H., Daley, G.Q., and Tang, D.G. (2009). Functional evidence that the self-renewal gene NANOG regulates human tumor development. Stem cells *27*, 993-1005.

Kassahun, W.T., Fangmann, J., Harm, J., Hauss, J., and Bartels, M. (2006). Liver resection and transplantation in the management of hepatocellular carcinoma: a review. Ex. Clin. Transplant. *4*, 549–558.

Kristiansen, G., Denkert, C., Schlüns, K., Dahl, E., Pilarsky, C., and Hauptmann, S. (2002). CD24 is expressed in ovarian cancer and is a new independent prognostic marker of patient survival. Am. J. Pathol. *161*, 1215–1221.

Kristiansen, G., Winzer, K.J., Mayordomo, E., Bellach, J., Schlüns, K., Denkert, C., Dahl, E., Pilarsky, C., and Altevogt, P. (2003). CD24 expression is a new prognostic marker in breast cancer. Clin. Cancer Res. *9*, 4906–4913.

Kuvshinoff, B.W., and Ota, D.M. (2002). Radiofrequency ablation of liver tumors: influence of technique and tumor size. Surgery *132*, 605–611.

Lapidot, T., Sirard, C., Vormoor, J., Murdoch, B., Hoang, T., Caceres-Cortes, J., Minden, M., Paterson, B., Caliqiuri, M.A., and Dick, J.E. (1994). A cell initiating human acute myeloid leukaemia after transplantation into SCID mice. Nature *367*, 645-648.

Li, C., Heidt, D.G., Dalerba, P., Burant, C.F., Zhang, L., Adsay, V., Wicha, M., Clarke, M.F., and Simeone, M. (2007). Identification of pancreatic cancer stem cells. Cancer Res. *67***,** 1030–1037.

Lin, L., Amin, R., Gallicano, G.I., Glasgow, E., Jogunoori, W., Jessup, J.M., Zasloff, M., Marshall, J.L., Shetty, K., and Johnson, L., et al. (2009). The Stat3 inhibitor NSC 74859 is effective in hepatocellular cancers with disrupted TGF-beta signaling. Oncogene *28*, 961-972.

Liu, S., Dontu, G., and Wicha, M.S. (2005). Mammary Stem cells, self-renewal pathways, and carcinogenesis. Breast Cancer Res. *7*, 86-95.

Llovet, J.M., and Bruix, J. (2003). Systematic review of randomized trials for unresectable hepatocellular carcinoma: chemoembolization improves survival. Hepatology *37*, 429–442.

Ma, S., Chan, K.W., Hu, L., Lee, T.K., Wo, J.Y., Ng, I.O., Zheng, B.J., and Guan, X.Y. (2007). Identification and characterization of tumorigenic liver cancer stem/progenitor cells. Gastroenterology *132*, 2542-2556.

Ma, S., Lee, T.K., Zheng, B.J., Chan, K.W., and Guan, X.Y. (2008). CD133+ HCC cancer stem cells confer chemoresistance by preferential expression of the Akt/PKB survival pathway. Oncogene *27*, 1749-1758.

Ma, S., Tang, K.H., Chan, Y.P., Lee, T.K., Kwan, P.S., Castilho, A., Ng, I.O., Man, K., Wong, N., and To, K.F., et al. (2010). miR-130b promotes CD133(+) liver tumor-initiating cell growth and self-renewal via tumor protein 53-induced nuclear protein 1. Cell Stem Cell *7*, 694-707.

Marquardt, J.U., and Thorgeirsson, S.S. (2010). Stem cells in hepatocarcinogenesis: evidence from genomic data. Semin. Liver Dis. *1*, 26-34.

Mattison, J., Kool, J., Uren, A.G., de Ridder, J., Wessels, L., Jonkers, J., Bignell, G.R., Butler, A., Rust, A.G., and Brosch, M., et al. (2010). Novel candidate cancer genes identified by a large-scale cross species comparative oncogenomics approach. Cancer Res. *70*, 883-895.

O'Brien, C.A., Pollett, A., Gallinger, S., and Dick, J.E. (2007). A human colon cancer cell capable of initiating tumor growth in immunodeficient mice. Nature *445*, 106–110.

Pardal, R., Clarke, M.F., and Morrison, S.J. (2003). Applying the principles of stem-cell biology to cancer. Nat. Rev. Cancer *3*, 895–902.

Patrawala, L., Calhoun, T., Schneider-Broussard, R., Zhou, J., Claypool, K., and Tang, D.G. (2005). Side population is enriched in tumorigenic, stem-like cancer cells, whereas ABCG2+ and ABCG2− cancer cells are similarly tumorigenic. Cancer Res. *65*, 6207–6219.

Pirruccello, S.J., and LeBien, T.W. (1986). The human B cell-associated antigen CD24 is a single chain sialoglycoprotein. J. Immunol. *136*, 3779–3784.

Sammar, M., Gulbins, E., Hilbert, K., Lang, F., and Altevogt, P. (1997). Mouse CD24 as a signaling molecule for integrin-mediated cell binding: functional and physical association with src-kinase. Biochem. Biophys. Res. Commun. *234*, 330-334.

Silva, J., Nichols, J., Theunissen, T.W., Guo, G., van Oosten, A.L., Barrandon, O., Wray, J., Yamanaka, S., Chambers, I., and Smith, A. (2009). Nanog is the gateway to the pluripotent ground state. Cell *138*, 7227-7237.

Singh, S.K., Clarke, I.D., Terasaki, M., Bonn, V.E., Hawkins, C., Squire, J., and Dirks, P.B. (2003). Identification of a cancer stem cell in human brain tumors. Cancer Res. *63*, 5821–5828.

Suzuki, A., Raya, A., Kawakami, Y., Morita, M., Matsui, T., Nakashima, K., Gage, F.H., Roddriguez-Esteban, and Izpisua Belmonte, J.C. (2006). Nanog binds to Smad1 and clocks bone morphogenetic protein-induced differentiation of embryonic stem cells. Proc. Natl. Acad. Sci. USA *103*, 10294-10299.

Tang, Y., Kitisin, K., Jogunoori, W., Li, C., Deng, C.X., Mueller, S.C., Ressom, H.W., Rashid, A., He, A.R., and Mendelson, J.S., et al. (2008). Progenitor/stem cells give rise to liver cancer due to aberrant TGF-beta and IL-6 signaling. Proc. Natl. Acad. Sci. USA *105*, 2445-2450.

Wang, M., Xiao, J., Shen, M., Yahong, Y., Tian, R., Zhu, F., Jiang, J., Du, Z., Hu, J., and Liu, W., et al. (2010). Isolation and characterization of tumorigenic extrahepatic cholangiocarcinoma cells with stem cell-like properties. Int. J. Cancer *128*, 72-81.

Woo, H.G., Park, E.S., Cheon, J.H., Kim, J.H., Lee, J.S., Park, B.J., Kin, W., Park, S.C., Chung, Y.J., and Kim, B.G., et al. (2008). Gene expression-based recurrence prediction of hepatitis B virus-related human hepatocellular carcinoma. Clin. Cancer Res. *14*, 2056-2064.

Yamashita, T., Ji, J., Budhu, A., Forgues, M., Yang, W., Wang, H.Y., Jia, H., Ye, Q., Qin, L.X., and Wauthier, E. et al (2009). EpCAM-positive hepatocellular carcinoma cells are tumor-initiating cells with stem/progenitor cell features. Gastroenterology *136*, 1012-1024.

Yang, X.R., Xu, Y., Yu, B., Zhou, J., Li, J.C., Qiu, S.J., Shi, Y.H., Wang, X.Y., Dai, Z., and Shi, G.M., et al. (2009). CD24 is a novel predictor for poor prognosis of hepatocellular carcinoma after surgery. Clin. Cancer Res. *15*, 5518-5527.

Yang, Z.F., Ho, D.W., Ng, M.N., Lau, C.K., Yu, W.C., Ngai, P., Chu, P.W., Lam, C.T., Poon, R.T., and Fan, S.T. (2008). Significance of CD90+ cancer stem cells in human liver cancer. Cancer Cell

13, 153-166.

Yeung, T.M., Gandhi, S.C., Wilding, J.L., Muschel, R., and Bodmer, W.F. (2010). Cancer stem cells from colorectal cancer-derived cell lines. Proc. Natl. Acad. Sci. USA *107*, 3722-3727.

Yu, F., Yao, H., Zhu, P., Zhang, X., Pan, Q., Gong, C., Huang, Y., Hu, X., Su, F., and Lieberman, J. et al. (2007). Let-7 regulates self-renewal and tumorigenicity of breast cancer cells. Cell *131*, 1109-1123.

Figure Legends

Figure 1. Up-regulation of CD24 in self-renewing liver cancer cells in chemoresistant HCC xenograft model. (A) Nude mice with xenograft tumors of 4 mm in diameter were separated into 4 groups and given different dosages (1 mg/kg, 2 mg/kg, 5 mg/kg, and no-drug control) of cisplatin at embedded intervals of 4 days for 4 weeks. (B) The dosage of 5 mg/kg was found to be optimal to achieve enrichment of chemoresistant cells, because further administration of drug from day 14 onwards did not cause significant shrinkage of the tumors, indicating that the majority of cells remaining in the small tumors were insensitive to cisplatin. (C) When the cells dissociated from the 'resistant group' and 'untreated group' tumors were injected orthotopically into secondary SCID mice recipients, 5×10^4 cells from the 'resistant group' were sufficient to form tumors, whereas no tumors were formed from the 'untreated group' cells. (D) By qPCR, it was shown that *CD24* was 2.9-fold higher in the PLC/PRF/5-derived 'resistant group' tumor cells. (E) Similarly, higher expression of CD24 at the protein level was shown by IHC analysis of paraffin-embedded tumor tissue. CD24-positivity in the PLC/PRF/5 and Huh-7 derived tumor was found to be increased in the 'chemoresistant group' when compared with the 'untreated group'. See also Figure S1. (F) By FACS analysis, it was found that MIHA, a non-tumorigenic liver cell line, did not express CD24, whereas the HCC cell lines tested varied in their expression levels, ranging from 6.4±2.6% in MHCC-97L to 97.7±1.5% in Huh-7 cells. (G &H) By IHC, it was shown that in clinical specimens, the non-tumorous liver tissues away from the HCC tumors stained negative for CD24, whereas in the tumorous tissues the expression of CD24 was scarce (29/41, i.e. 70.7% of cases examined had <2% positivity) and usually in few isolated cells. Error bars represent standard deviation (SD) from at least three independent experiments.

Figure 2. $CD24^+$ HCC cells possessed traits of stem/progenitor cells. (A) Representative images of the primary-sorted PLC/PRF/5 and HLE and secondary PLC/PRF/5 cell-induced tumor formation. See also Table S1. Right flanks were injected with $CD24^+$ cells while left flanks were

injected with $CD24^-$ cells. Red arrow indicates the site of tumor formation for HLE cells (B) Paraffin-embedded tissue of the xenotransplanted tumors were processed for H&E staining and IHC to detect CD24 expression. These representative images show that in cases of tumor formation, tumor cell heterogeneity, in terms of both cell morphology and CD24 expression, was observable. (C) By sphere forming assay, the *in vitro* self-renewal ability was enhanced in $CD24^+$ cells from PLC/PRF/5 and HLE (left column). Secondary spheres formed from dissociating both spheres also demonstrated enhanced serial sphere-forming capacity in $CD24^+$ cells, respectively (right column). (D) By colony formation assay on the sorted cells of PLC/PRF/5 and HLE), it was demonstrated that $CD24^+$ HCC cells had a significantly lower proliferation rate when compared with $CD24^-$ cells respectively ($*P$ <0.010 and $*P$ <0.001, respectively, *t* test). (E) $CD24^+$ cells from the two HCC cell lines, PLC/PRF/5 and HLE, overexpressed several genes related to 'stemness' when compared to $CD24^-$ cells. (∗p<0.05; ∗∗p<0.01) Error bars represent standard deviation (SD) from at least three independent experiments.

Figure 3. Clinical relevance of CD24 expression. (A) When cells from a fresh clinical HCC sample (Patient #38) were sorted magnetically into $CD24^+$ and $CD24^-$ fractions, the $CD24^+$ cells displayed significantly enhanced anchorage-independent growth in the soft-agar colony formation assay, indicating higher *in vitro* tumorigenicity. (B) As few as 4000 $CD24^+$ HCC cells (4/4) from two clinical HCCs induced tumor formation. Right flanks were injected with $CD24^+$ cells while left flanks were injected with $CD24^-$ cells. Red arrows indicate the site of tumor formation. (C) Paraffin-embedded tissues of the xenotransplanted tumors were processed for H&E staining and IHC to detect CD24 expression. (D) $CD24^+$ cells from primary HCC samples overexpressed several genes related to 'stemness' when compared with $CD24^-$ cells. (∗p<0.05; ∗∗p<0.01) (E). By sphere forming assay, the *in vitro* self-renewal ability was enhanced in $CD24^+$ cells from fresh HCC tumor (Patients #36, #38 and #51). (F) Kaplan-Meier curves for disease-free and overall survival were compared according to the *CD24* expression in tumor tissues. The overall and disease-free survival

of HCC patients with *CD24* overexpression in their tumors were 36.7 and 6.6 months as compared with 94.2 and 42.4 months in patients with low *CD24* expression (P=0.113 and 0.002, respectively, log-rank test). Error bars represent standard deviation (SD) from at least three independent experiments.

Figure 4. $CD24^+$ HCC cells had the capacity to differentiate and metastasize i*n vivo.* (A&B) Using trans-well migration and invasion assays, it was shown that the $CD24^+$ fraction of sorted PLC/PRF/5 cells had enhanced migratory ($*P$<0.001, *t* test) and invasive properties ($*P$<0.001, *t* test) *in vitro*. (C&D) By experimental metastatic assay in NOD/SCID mice which was evaluated by bioluminescent imaging, it was found that $CD24^+$ PLC/PRF/5 cells injected intravenously successfully colonized the lungs in 3 of 5 mice, whereas the $CD24^-$ cells did not colonize, indicating enhanced *in vivo* metastatic ability. (E) By immunofluorescence staining, spheres of stem-like cells derived from clinical HCC cells displayed strong expression of CD24, and CD24 expression (green color) was lost and CK18 (marker for differentiated hepatoyctes; red color) was gained near peripheral region upon differentiation. The cells are counterstained with DAPI. (F&G) By comparing the gene expression of spheres of stem-like cells with their differentiated progenies, it was found that, for both PLC/PRF/5 cell line and clinical HCC cells (Patient #3), CD24 expression was relatively higher in the spheres than in the parental cells. The 'stemness' of the spheres was also reflected by the overexpression of several 'stemness'-associated genes. (H) Upon culture in serum-containing medium for 2 weeks, FACS-sorted $CD24^+$ PLC/PRF/5 cells gradually reconstituted the original proportion of CD24-expressing cells, whereas $CD24^-$ cells failed to give rise to the original heterogeneity of CD24 expression. Error bars represent standard deviation (SD) from at least three independent experiments. See also Figures S2, S3 and S4.

Figure 5. CD24 knockdown reduced characteristics of liver T-ICs. (A&B) Knockdown of CD24 in Huh-7 and PLC/PRF/5 cells resulted in down-regulation of several genes related to

'stemness' as compared to the non-target control (NTC). (∗p<0.05; ∗∗p<0.01, *t* test) (C) CD24 knockdown (shCD24) HCC cells exhibited reduced tumor-forming incidence when compared with NTC cells. See also Table S2. Right flanks were injected with NTC cells while left flanks were injected with shCD24 cells. Corresponding paraffin-embedded tissue of the xenotransplanted tumors were processed for H&E staining and IHC to detect CD24 expression. (D) The effect of CD24 knockdown on tumorigenicity of PLC/PRF/5 cells was evaluated using xenogen bioluminescence imaging. Representative image of tumor developed from PLC/PRF/5 cells derived from NTC (left) and shCD24 (right) and corresponding paraffin-embedded tissue of the xenotransplanted tumors were processed for H&E staining and IHC to detect CD24 expression. (E) H & E staining of paraffin-embedded lung tissue from SCID mice after orthotopic injection of NTC cells. Black arrows indicate the tumor foci within the lung tissue. (F) Knockdown of CD24 in Huh-7 and PLC/PRF/5 cells resulted in significant increase in proliferative rate respectively (∗*P*=.017 and ∗*P*=.032, respectively, *t* test). (G) Knockdown of CD24 also reduced the size and number of hepatospheres formed in Huh-7 and PLC/PRF/5 cells (*P*<0.001, *t* test). In addition, knockdown of CD24 decreased the ability of cells to form secondary hepatospheres (*P*<0.001, *t* test). Error bars represent standard deviation (SD) from at least three independent experiments. See also Figure S5.

Figure 6. CD24 drove tumor formation and self-renewal via Stat3-mediated *Nanog* regulation. (A) *Nanog* expression in different HCC cell lines was evaluated by qPCR and found to significantly correlate with CD24 expression (*P*=0.012, r= 0.955, Pearson's Correlation). (B). *CD24* expression significantly correlated with *Nanog* expression in 46 HCC patients (*P*=0.026, r=0.325, Pearson's Correlation). (C) *Nanog* was successfully transfected in a CD24 knockdown clone (#278) of Huh-7 cells and the expression level was comparable to the non-target control. (D) The tumorigenicity of CD24 knockdown cells increased upon *Nanog* transfection. Representative image of tumor developed from Huh-7 derived from shCD24 (left) and shCD24-*Nanog* (right). (E)

In addition, *Nanog* overexpression in shCD24 knockdown cells also increased the sizes of and number of hepatospheres formed in Huh-7 and PLC/PRF/5 cells ($P<0.001$, *t* test). In addition, *Nanog* overexpression increased the ability of cells to form primary and secondary hepatospheres in shCD24 cells respectively ($P<0.001$, *t* test). (F) Decreased level of phosphorylated Stat3 (Y705) but not its parental form was observed after CD24 knockdown in Huh-7 and PLC/PRF/5 cells. (G) Quantitative assessment of GFP-positive cells by flow cytometry for *Nanog* promoter activity. Flow cytometry analysis showed a 4.5-fold increase in the percentage of GFP-positive cells in $CD24^+$ PLC/PRF/5 cells when compared with $CD24^-$ cells, and its percentage decreased after incubation of S3I-201 at 200 μM. Immunofluorescence staining also revealed increase of GFP signal in $CD24^+$ cells when compared with its $CD24^-$ counterpart. (H) A marked decrease of pStat3 bound on the upstream of transcriptional start site of Nanog was found upon CD24 knockdown Huh-7 and PLC/PRF/5 cells as compared with the corresponding vector control in ChIP assay. Normal rabbit antibody added served as a negative control. Error bars represent standard deviation (SD) from at least three independent experiments. See also Figures S6 and S7 and Tables S3, S4 and S5.

Figure 1

Click here to download high resolution image

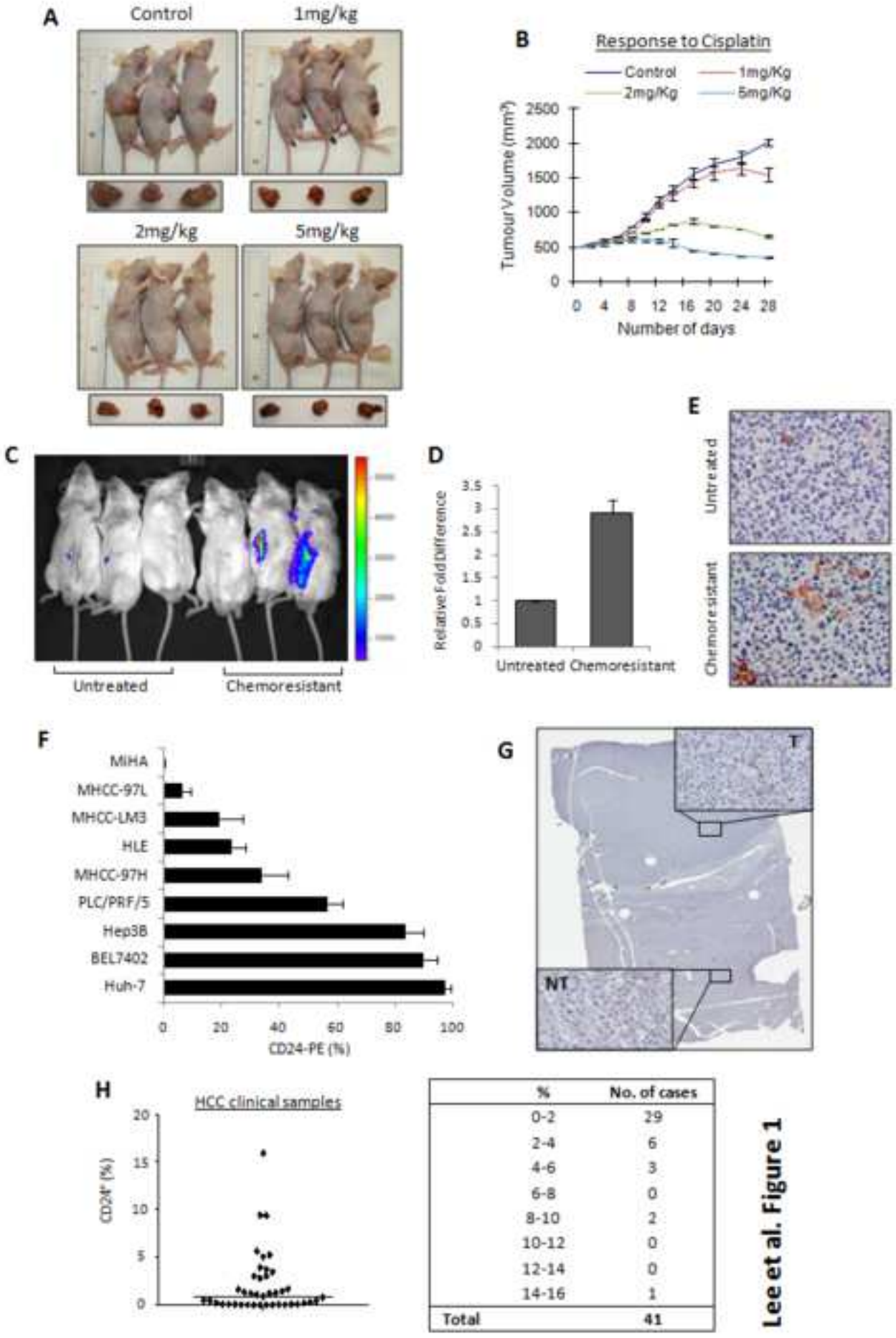

%	No. of cases
0-2	29
2-4	6
4-6	3
6-8	0
8-10	2
10-12	0
12-14	0
14-16	1
Total	41

Lee et al. Figure 1

Figure 2

Click here to download high resolution image

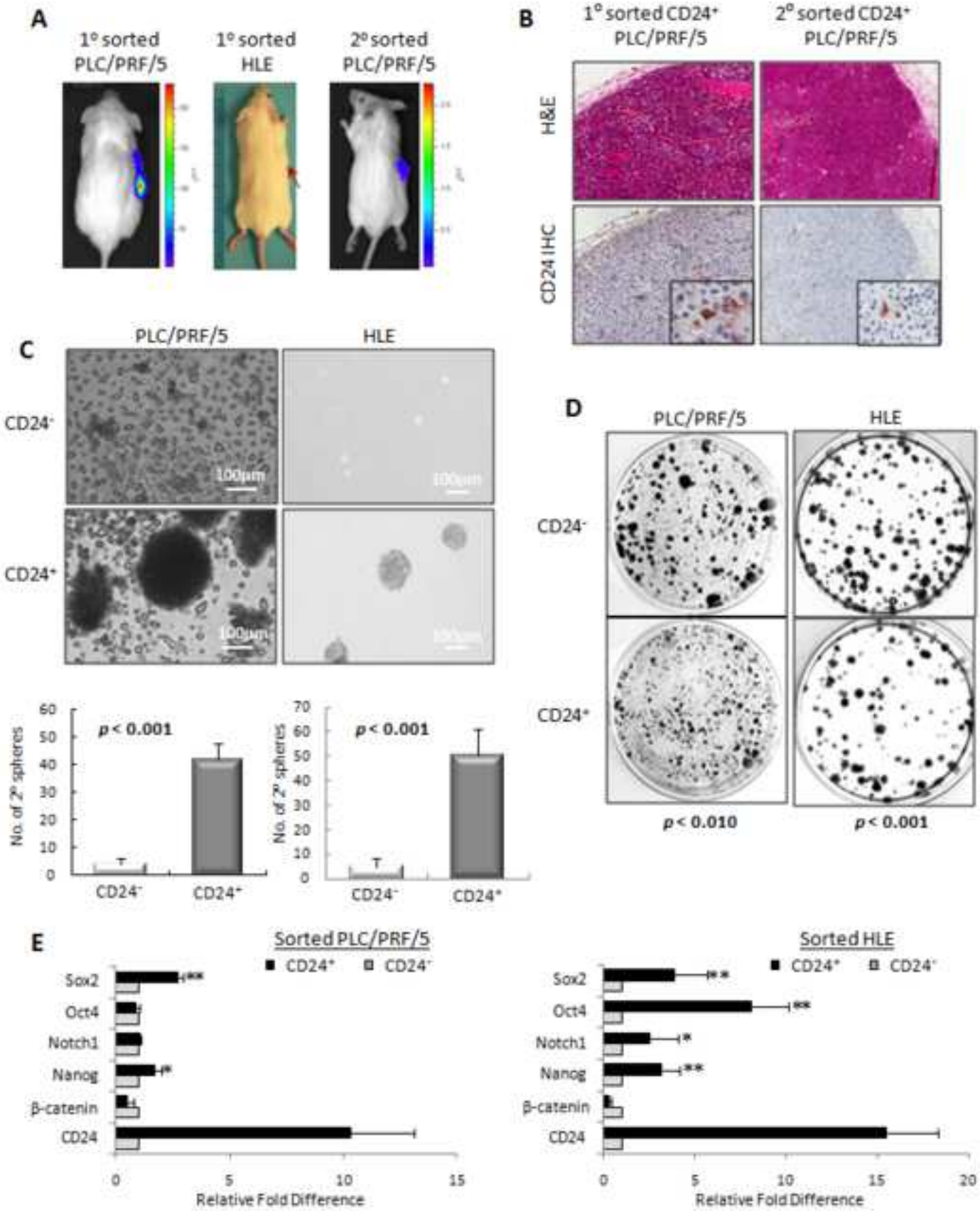

Lee et al. Figure 2

Figure 3

Click here to download high resolution image

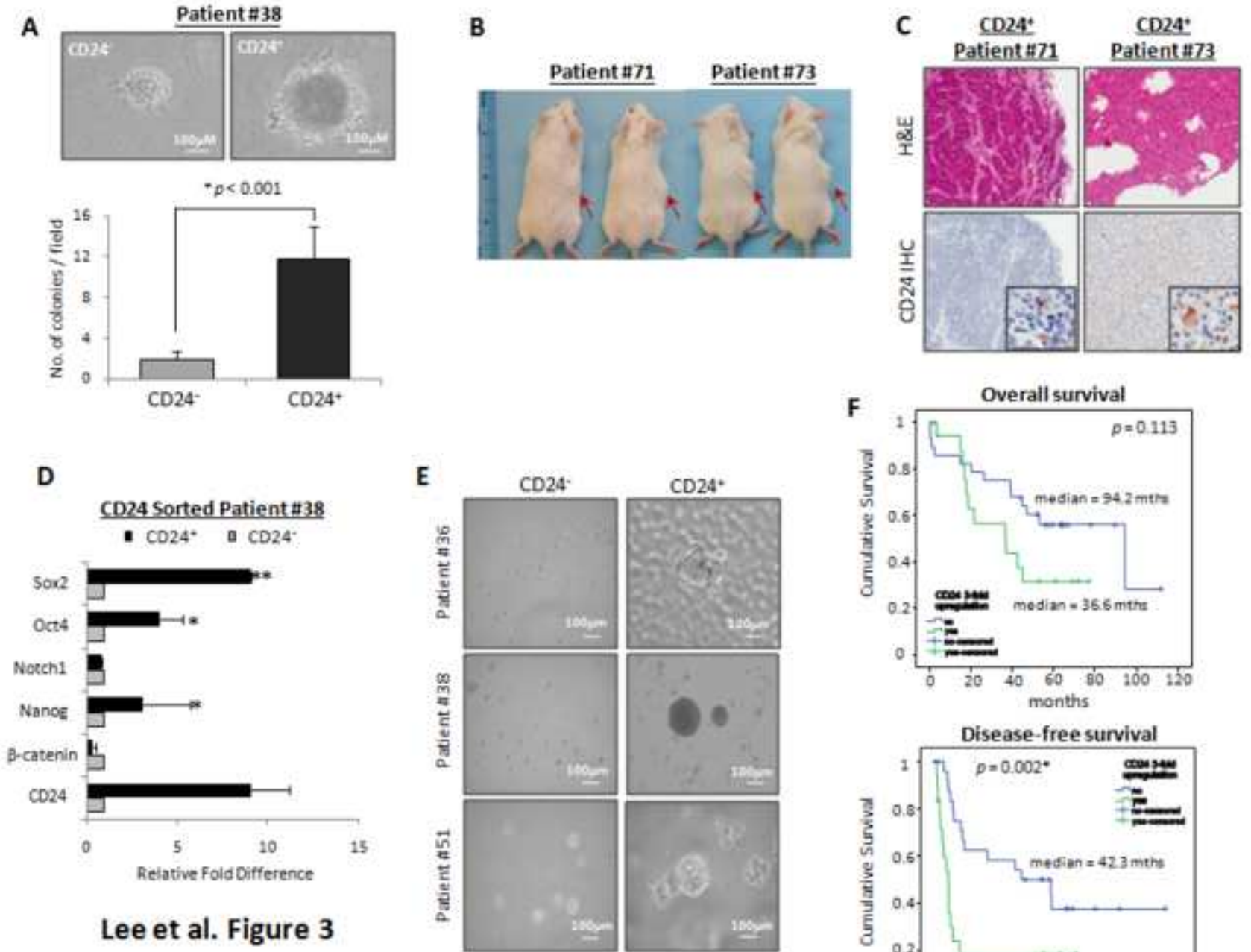

Lee et al. Figure 3

Figure 4

Click here to download high resolution image

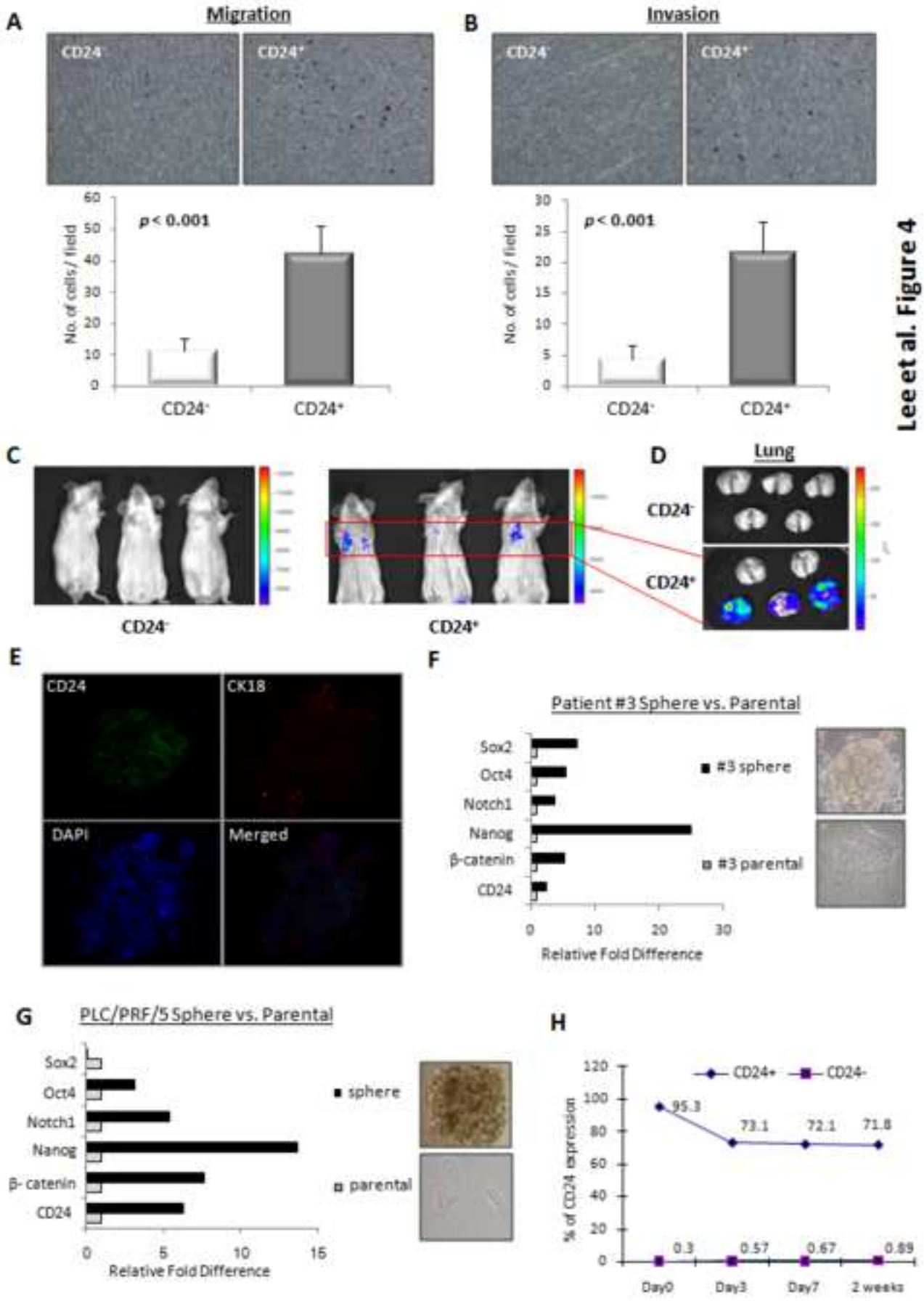

Lee et al. Figure 4

Figure 5

Click here to download high resolution image

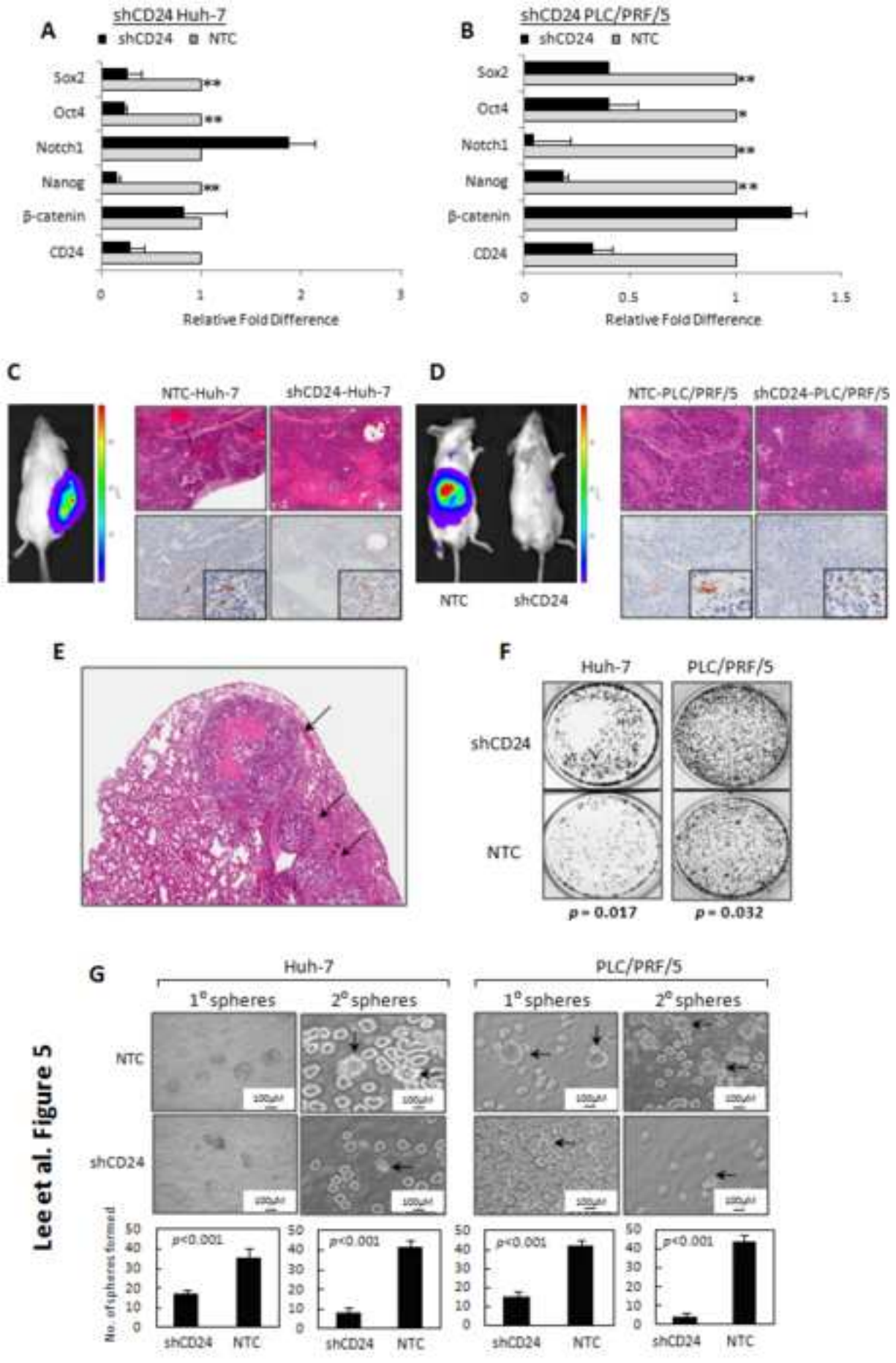

Lee et al. Figure 5

Figure 6

Click here to download high resolution image

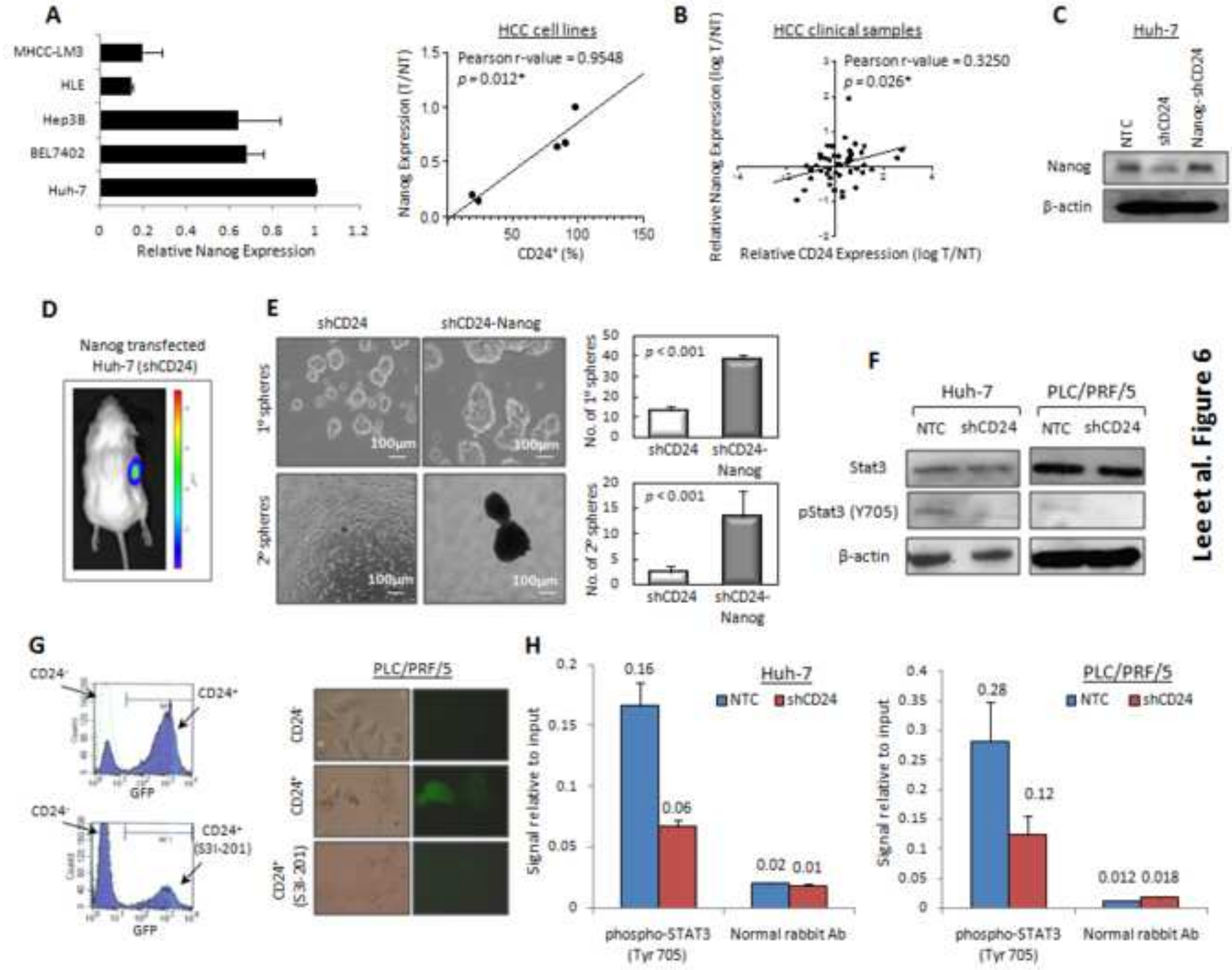

Table 1. Clinico-pathologic correlation of CD24 expression in HCC patients

Clinico-pathological variables	CD24 over-expression		*p*-value
	≤ 3-fold	> 3-fold	
Recurrence in the first year (*n* = 46)			
No	22	6	**0.002***†
Yes	6	12	
Venous infiltration (*n* = 43)			
Absence	19	3	**0.003***†§
Presence	9	12	
Serum AFP level (*n* = 36)			
Low (≤ 20 ng/ml)	16	4	**0.009***†§
High (> 20 ng/ml)	6	10	
TNM stage (*n* = 43)			
Early stage (I-II)	15	2	**0.010***†§
Late stage (III-IV)	13	13	
Microsatellites (*n* = 46)			
Absence	23	10	0.051†
Presence	5	8	
Age (*n* = 46)			
Young (≤ median, 54)	13	12	0.179†
Old (> median, 54)	15	6	
Differentiation status (*n* = 36)			
Well differentiated	7	3	0.456‡§
Moderately to poorly differentiated	13	13	
Tumor size (*n* = 45)			
Small (≤ 5 cm)	14	7	0.565†§
Large (> 5 cm)	14	10	
HBV association *(n* = 46)			
Negative of HBsAg	11	8	0.729†
Positive of HBsAg	17	10	

∗ Significant difference
‡ Fisher's exact test
† χ^2 test
§ Total number <46 due to missing data

CD24$^+$ liver tumor-initiating cells drive self-renewal and tumor initiation through Stat3-mediated Nanog regulation

Terence Kin Wah Lee, Antonia Castilho, Vincent Chi Ho Cheung, Kwan Ho Tang, Stephanie Ma, Irene Oi Lin Ng

Inventory of Supplemental Information

$CD24^+$ liver tumor-initiating cells drive self-renewal and tumor initiation through Stat3-mediated Nanog regulation

Terence Kin Wah Lee, Antonia Castilho, Vincent Chi Ho Cheung, Kwan Ho Tang, Stephanie Ma, Irene Oi Lin Ng

Supplemental Figures and Legends

Figure S1. **Up-regulation of CD24 in a chemoresistant HCC xenograft model derived from Huh-7 cells. (A)** Cisplatin at 5 mg/kg was administered to nude mice carrying tumors derived from the cell line Huh-7. **(B)** CD24 was found to be overexpressed in the "resistant group" of Huh-7-derived tumors upon IHC analysis. Related to Figure 1.

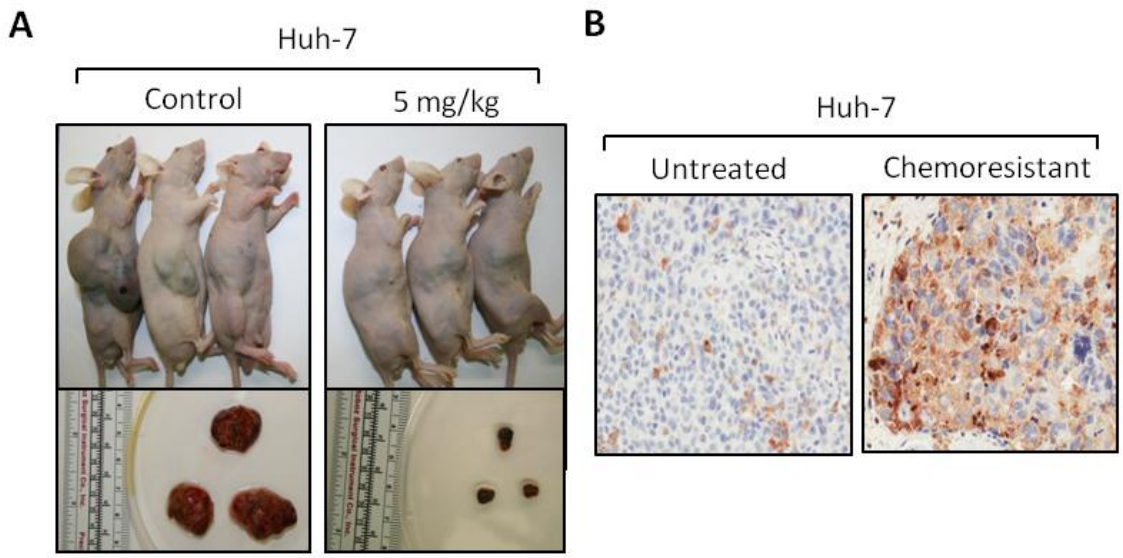

Lee et al. Figure S1

Figure S2. **Histological analysis of lung and skin of NOD/SCID mice. (A)** Histological analysis showed lung metastasis after subcutaneous inoculation of $CD24^+$ cells derived from patient #71 and #73. **(B)** Lack of tumorigenicity in the skin of NOD/SCID mice inoculated with $CD24^-$ cells derived from patient #71. Related to Figure 4.

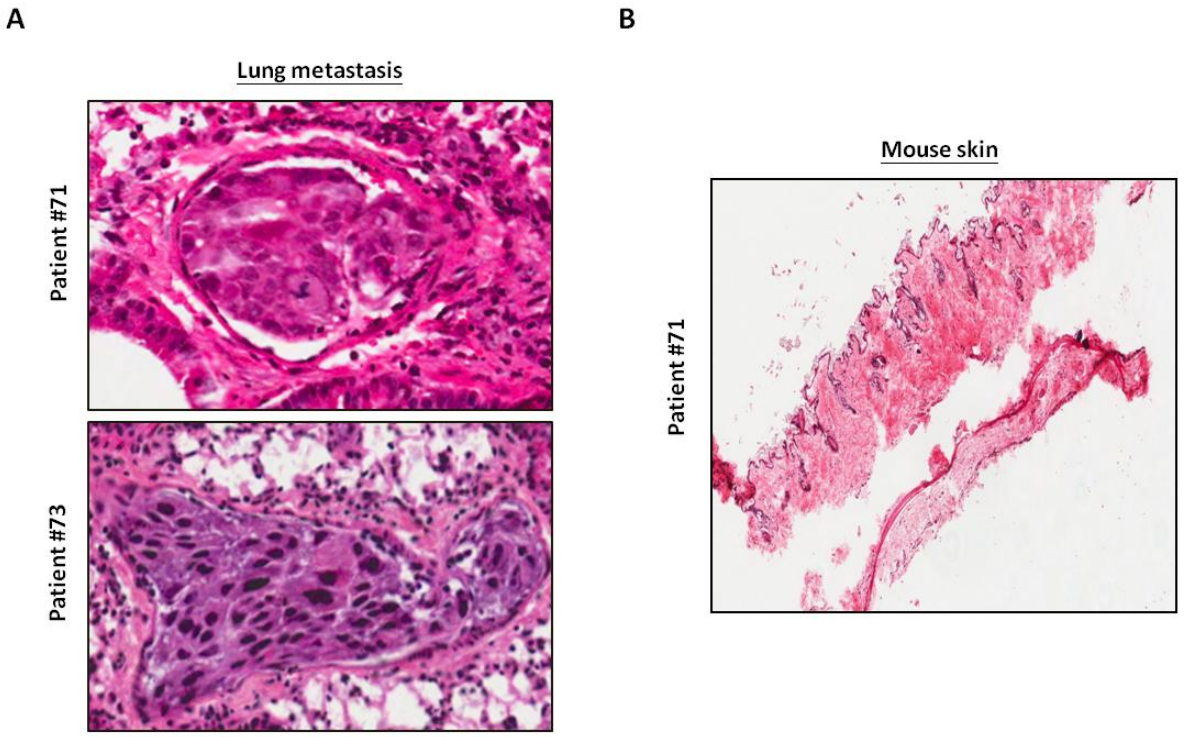

Figure S3. **CD24 serves unique function in T-IC of HCC. (A)** CD24 expression significantly overlapped with the expression of the markers CD133 and EpCAM. By FACS analysis on Huh-7 cells, the majority of $CD24^+$ cells expressed the two other reported HCC T-IC markers, EpCAM (55.8%) and CD133 (90.9%). 100% $EpCAM^+$ cells were $CD24^+$, and 98.9% $CD133^+$ cells were $CD24^+$. **(B)** CD90 was knocked down in MHCC-97H cells by lentiviral based approach. **(C)** As few as 500 $CD24^+$ HCC cells from MHCC-97H induced tumor formation. Right flanks were injected with $CD24^+$ cells while left flanks were injected with $CD24^-$ cells. Black arrows indicate the site of tumor formation. Tumorigenicity of $CD24^+$ cells is comparable between CD90 knockdown cells (75%) and control cells (83.3%). Related to Figure 4.

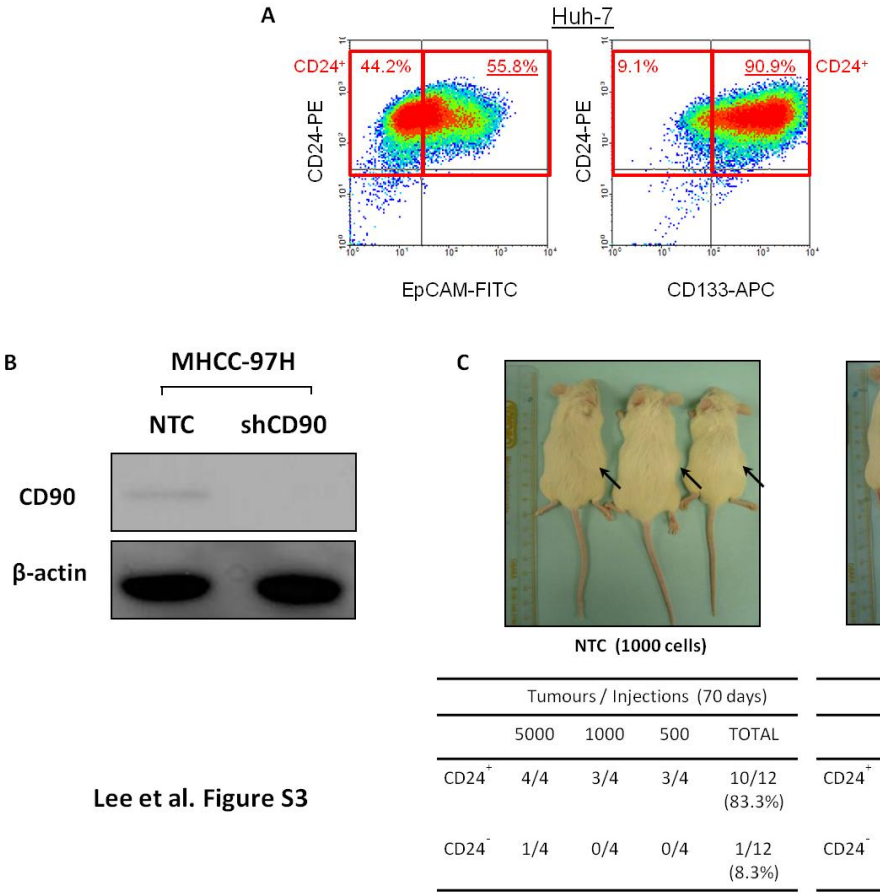

	Tumours / Injections (70 days)			
	5000	1000	500	TOTAL
$CD24^+$	4/4	3/4	3/4	10/12 (83.3%)
$CD24^-$	1/4	0/4	0/4	1/12 (8.3%)

	Tumours / Injections (70 days)			
	5000	1000	500	TOTAL
$CD24^+$	4/4	3/4	2/4	9/12 (75%)
$CD24^-$	1/4	0/4	0/4	1/12 (8.3%)

Lee et al. Figure S3

Figure S4. Differentiation capacity of CD24$^+$ HCC cells by single cell sorting approach. CD24$^-$ and CD24$^+$ single cells from PLC/PRF/5 cells were isolated by single cell sorting. Corresponding cells are seeded onto 96 well plates and grown in 10% FBS supplemented medium. After 3 weeks, CK18 expression was evaluated by Cells-to CT™ kit (Applied Biosystems, Foster city, CA). CK18 was 4 fold more in CD24$^+$ cells when compared with CD24$^-$ cells. Upon differentiation, there is no apparent increase in CK18 expression in CD24$^-$ cells while there is 3.69-fold increase in CK18 expression in CD24$^+$ cells. Error bars represent standard deviation (SD) from at least three independent experiments. Related to Figure 4.

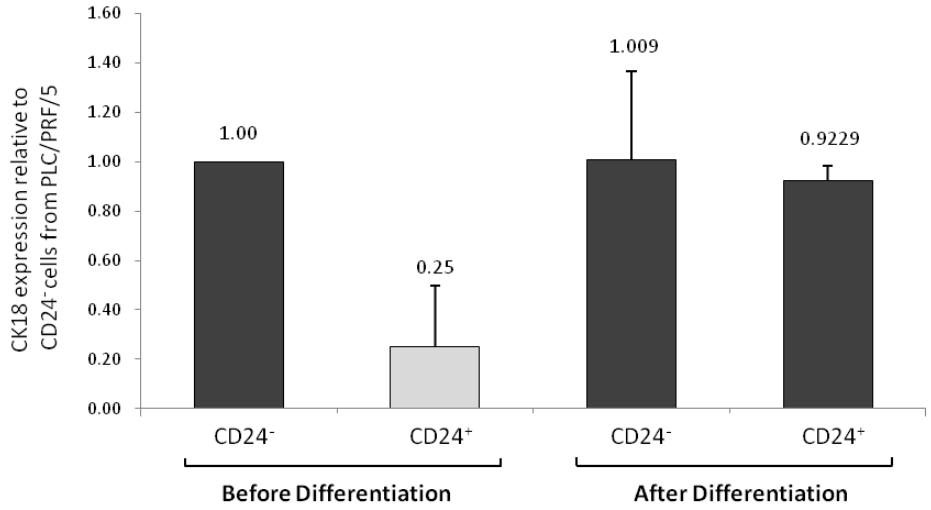

Lee et al. Figure S4

Figure S5. The effect of CD24 altered expression on chemosensitivity of HCC cells. (A) Upon CD24 knockdown in Huh-7 cells, CD24 knockdown cells are more chemosensitive to cisplatin (27.3% vs 12.3%) and doxorubicin (39.3% vs 24.4%) when compared with control cells after treatment for 24 hours at 5 µg/mL and 3 µg/mL respectively. **(B)** By Annexin V staining, $CD24^+$ cells derived from PLC/PRF/5 is more chemoresistant to cisplatin (35.4% vs 71.1%) and doxorubicin (38.6% vs 78.2%) when compared with $CD24^-$ cells after treatment for 24 hours at 10 µg/mL and 6 µg/mL, respectively. Related to Figure 5.

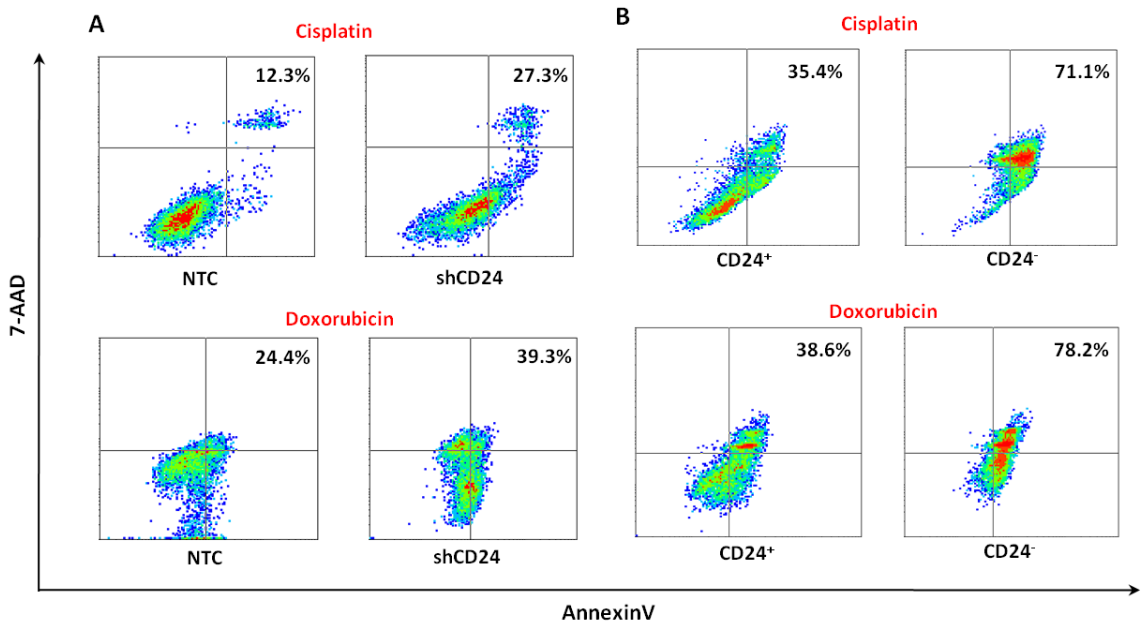

Lee et al. Figure S5

Figure S6. Significance of Stat3 phosphorylation in CD24 signaling pathway. (A) Poor correlation between *Sox2* and CD24 expression in the HCC cell lines. **(B)** Ingenuity Pathway analysis showed 8 most significant canonical pathways altered upon CD24 knockdown in Huh-7 cells. **(C)** Ingenuity Pathway analysis demonstrated the significance of Stat3 in IL-6 pathway upon knockdown of CD24 in Huh-7 cells. Error bars represent standard deviation (SD) from at least three independent experiments. Related to Figure 6.

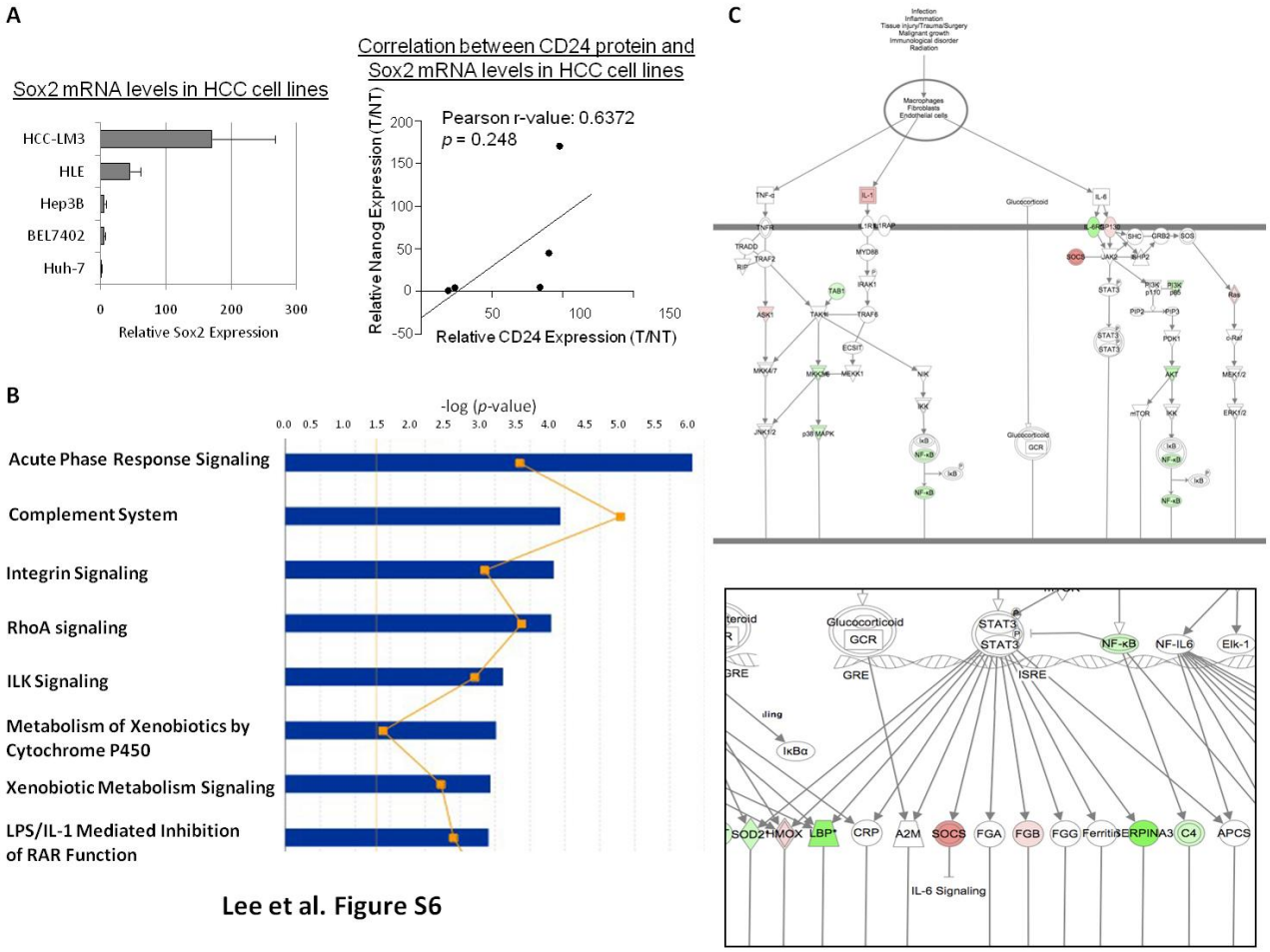

Lee et al. Figure S6

Figure S7. **CD24 phosphorylates Stat3 (Y705) through Src. (A)** Levels of phosphorylated Stat3 (Y705) and Nanog were down-regulated in dose-dependent manner upon administration of S3I-201. **(B)** CD24 ORF was transfected into CD24 negative MIHA cells. Levels of phosphorylated Stat3 (Y705) and Nanog were up-regulated but this effect was abolished upon administration of S3I-201 in dose-dependent manner. **(C)** pY416-Src, an active form of Src, but not JAK2 was decreased upon CD24 knockdown in Huh-7 and PLC/PRF/5 cells. **(D)** pY416-Src but not JAK2 and its phosphorylated form was increased upon CD24 overexpression in MIHA cells. **(E)** Addition of JAK inhibitor at 50μM did not overcome the increase of pStat3 (Y705) in CD24 overexpressing MIHA cells, which suggests that CD24 did not phosphorylate Stat3 through JAK2. Related to Figure 6.

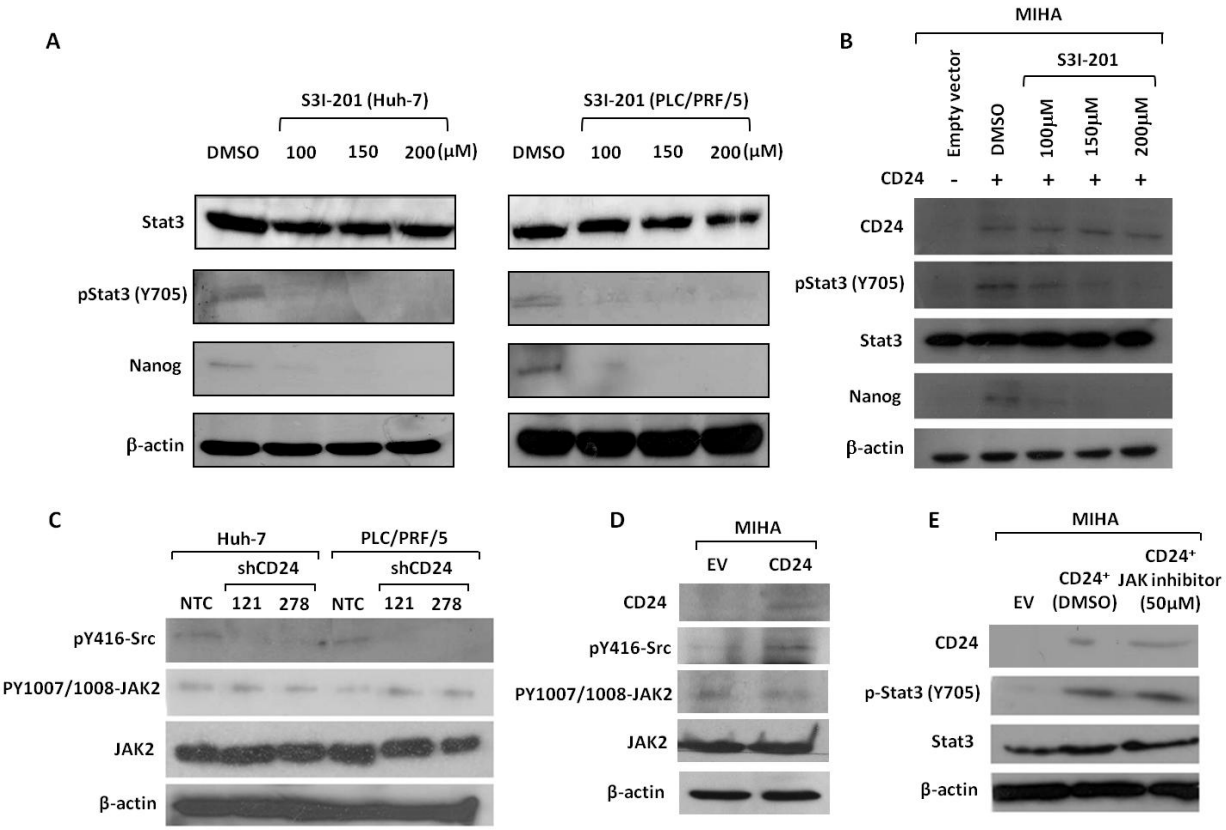

Lee et al. Figure S7

Supplemental Tables

Table S1. Tumorigenicity of CD24$^-$ and CD24$^+$ HCC cells in NOD/SCID mice. (A) Subcutaneous *in vivo* tumor development by CD24$^-$ and CD24$^+$ cells sorted from PLC/PRF/5 in NOD/SCID mice. **(B)** *In vivo* tumor development experiments of CD24$^-$ and CD24$^+$ cells sorted from HLE in NOD/SCID mice. **(C)** Subcutaneous *in vivo* tumor development of serially transplanted CD24$^-$ and CD24$^+$ cells sorted from CD24$^+$ HCC cell-derived xenograft tumors in NOD/SCID mice. Related to Figure 2.

A **Primary engraftment of sorted PLC/PRF/5 cells**

	Tumors / Injections						
	$1x10^5$	$5x10^4$	$2x10^4$	5000	1000	500	TOTAL
CD24$^+$	2/2	4/4	5/6	5/6	6/6	5/6	27/30 (90%)
Latency (days)	25	25	30	50	50	50	
CD24$^-$	1/2	2/4	2/6	1/6	0/6	0/6	6/30 (20%)
Latency (days)	30	40	40	45	-	-	

B **Engraftment of sorted HLE cells**

	Tumors / Injections				
	$1x10^5$	$5x10^4$	5000	500	TOTAL
CD24$^+$	2/2	3/4	4/6	3/6	12/18 (66.7%)
Latency (days)	40	50	70	80	
CD24$^-$	0/2	0/4	0/6	0/6	0/18 (0%)
Latency (days)	-	-	-	-	

C **Secondary engraftment of sorted PLC/PRF/5 cells**

	Tumors / Injections					
	$2x10^5$	$2x10^4$	5000	1000	500	TOTAL
CD24$^+$	6/6	6/6	5/6	6/6	6/6	29/30 (96.7%)
Latency (days)	20	20	20	25	25	
CD24$^-$	3/6	1/6	0/6	0/6	1/6	5/30 (16.7%)
Latency (days)	30	30	-	-	50	

Table S2. *In vivo* tumor development of shCD24 and non-target control cells from Huh-7 in SCID mice. Related to Figure 5.

Engraftment of CD24-knockdown and non-target control Huh7 cells

	Tumors / Injections						
	$5x10^5$	$1x10^5$	$5x10^4$	$2x10^4$	1000	500	TOTAL
Non-target control cells	5/5	6/7	3/5	2/4	4/5	1/5	20/31 (65%)
Latency (days)	40	45	50	60	70	80	
shCD24 cells	3/5	1/7	2/5	0/4	0/5	1/5	7/31 (22%)
Latency (days)	40	45	50	-	-	80	

Table S3. Expression of stemness associated genes including *β-catenin*, *Nanog*, *Notch1*, *Sox2*, *Oct4*, *Nestin*, *Smo*, *Bmi-1*, *ABCB5*, *ABCG2*, *ABCB1*, *ABCC1*, and *ABCC2* in CD24 deficient cells by both cell sorting and knockdown approach. Related to Figure 6.

	β-catenin	Nanog	Notch1	Oct4	Sox2	Nestin	Smo	Bmi-1	ABCC1	ABCC2	ABCB5	ABCG2	ABCB1
Under-expression in $CD24^-$ fraction relative to $CD24^+$ counterparts													
CD24 - PLC/PRF/5	1.94	**0.58**	0.95	1.17	0.36	0.54	0.89	1.11	1.07	0.65	1.21	1.23	0.3
CD24 - HLE	3.36	**0.31**	0.39	0.12	0.25	0.98	0.66	1.53	1.4	0.87	0.05	0.87	0.8
CD24 - Patient #38	2.92	**0.32**	1.15	0.24	0.11	0.6	0.34	1.32	0.93	0.45	0.34	0.2	0.9
Down-regulation in shCD24 cells relative to non-target control cells													
shCD24 - Huh7	0.82	**0.15**	1.87	0.24	0.26	1.82	0.97	1.05	1.2	1.5	1.12	0.6	1.1
shCD24 - PLC/PRF/5	1.26	**0.18**	0.04	0.39	0.4	0.72	0.9	1.9	0.84	1.06	1.1	1.1	0.6
shCD24 - Hep3B	0.65	**0.49**	0.03	0.53	0.33	0.89	1.17	0.6	0.6	0.72	0.75	0.7	1.9
shCD24 - Patient #3	0.2	**0.06**	1.08	0.03	0.03	0.08	0.05	0.3	1.1	1.3	1.04	0.23	2.1

Table S4. **Correlation between *CD24* and *Nanog* expression in 46 HCC clinical samples.** Related to Figure 6.

	n = 46	*Nanog expression*		*p-value*
		<1.5-fold	*>=1.5-fold*	
CD24 expression				
<3-fold	25	19	6	**0.022***
>=3-fold	21	9	12	

Table S5. ***In vivo*** **tumor development experiments of shCD24 and Nanog-shCD24 cells from Huh-7 in SCID mice.** Related to Figure 6.

Engraftment of CD24-knockdown, Nanog-overexpressing CD24-knockdown, (and non-target control) Huh7 cells

	Tumors / Injections					
	$1x10^5$	$5x10^4$	$2x10^4$	1000	500	TOTAL
shCD24	2/3	0/3	0/6	1/6	0/6	3/24 (12.5%)
Latency (days)	45	-	-	70	-	
Nanog-shCD24	3/3	1/3	4/6	5/6	5/6	18/24 (75%)
Latency (days)	45	55	55	70	80	
Non-target control	6/7	3/5	2/4	4/5	1/5	16/26 (61.5%)

Supplemental Experimental Procedures

Cell lines and cell culture. The human HCC cell lines MHCC-97L, MHCC-97H, MHCC-LM3 (from Liver Cancer Institute, Fudan University, China) (Li et al., 1997), Huh-7, HLE, PLC/PRF/5 (Japanese Cancer Research Bank, Tokyo, Japan), and Hep3B (American type Culture Collection, HB-8064) were maintained in DMEM with high glucose (Gibco BRL, Grand Island, NY) supplemented with 10% heat-inactivated fetal bovine serum (Gibco BRL), 100 mg/mL penicillin G, and 50 μg/mL streptomycin (Gibco BRL) at 37°C in a humidified atmosphere containing 5% CO_2. MIHA was kindly provided by Dr. J.R. Chowdhury, Albert Einstein College of Medicine, New York (Brown et al., 2000).

Patient samples. Human HCC and corresponding non-tumorous liver samples were collected at the time of surgical resection at Queen Mary Hospital, the University of Hong Kong, from 2001 to 2003. After collection from surgical resection, all samples were immediately snap-frozen in liquid nitrogen before storage at -80°C.

Plasmids and reagents. Cisplatin was obtained from Calbiochem (La Jolla, CA) and Stat3 inhibitor (S3I-201) and JAK inhibitor I (sc-204021) were from Santa Cruz Biotechnology (Santa Cruz, CA). Lentiviral-based GFP tagged human *Nanog* promoter and was purchased from System Biosciences (Mountain View, CA). CD24 and *Nanog* ORF were purchased in GeneCopoeia (Rockville, MD) and GenTarget (San Diego, CA) respectively.

cDNA microarray. Total RNA was isolated using TRIZOL Reagent (Invitrogen, Carlsbad, CA) according to the manufacturer's instructions. The quality of total RNA was checked with an Agilent 2100 bioanalyzer. The RNA was then amplified and labeled with MessageAmp II-Biotin Enhanced Single Round RNA Amplification Kit (Ambion Inc., TX). In brief, double-stranded cDNA was generated by reverse transcription from 1 g of total RNA with an oligo(dT) primer bearing a T7 promoter. The double-strand cDNA was used as a template for in vitro transcription to generate biotin-labeled cRNA. After fragmentation, 15 g of cRNA was hybridized to the GeneChip array for 16 hr. The GeneChips were washed and stained using the GeneChip Fluidics Station 400 (Affymetrix Inc. Santa Clara, CA) and then scanned with the GeneChip Scanner 3000 (Affymetrix). Genome-wide expression profiles were analyzed by the gene chip system Human U133 Plus 2.0 (Affymetrix). RNA quality control, sample labeling, GeneChip hybridization, and data acquisition were performed at the Genome Research Centre, the University of Hong Kong. To compare the gene expression patterns, hybridization intensity in the samples was normalized with

the Affymetrix global scaling method (Affymetrix). Computational analyses were performed using Genespring gx v.11 software (Silicon Genetics). Scanned output files were analysed using Robust Multichip Average (RMA) methods with Genespring GX software, Affymetrix. Transcripts with more than a two-fold difference level were defined as differentially expressed. Microarray data are available publicly at http://www.ncbi.nlm.nih.gov/geo/(Geo accession number, GSE28057).

Lentiviral-based transfection into HCC cells. For luciferase labeling of HCC cells, Huh-7 and PLC/PRF/5 cells were labeled with luciferase using a lentiviral-based approach as previously described (Lee et al., 2007). For suppression of CD24 and CD90 in HCC cells, lentiviral particles (DFCI-Broad RNAi Consortium, Boston) expressing shRNAs against human CD24 and CD90 were used to downregulate *cd24* and *cd90* mRNA. Transduced cells were selected with 2 μg/mL puromycin.

Sphere formation assay. A total of 200 single HCC cells were plated onto 24-well polyHEMA (Sigma)-coated plates. Cells were grown in DMEM/F12 medium (Invitrogen, Carlsbad, CA) for 10 days supplemented with 4 μg/mL insulin (Sigma-Aldrich, St. Louis, MO), B27 (Invitrogen, Carlsbad, CA), 20 ng/mL EGF (Sigma-Aldrich, St. Louis, MO), and 20 ng/mL basic FGF (Invitrogen, Carlsbad, CA). For serial passage of primary spheres, the primary spheres were collected, subsequently dissociated with trypsin, and resuspended in DMEM/F12 medium with the above supplements.

Proliferation assay. Cells were seeded at a density of 1,000 cells per well and allowed to grow for five to seven days. Cell proliferation was assessed by a colorimetric assay using crystal violet as described previously (Ng et al., 2000).

Anchorage independent growth assay. Cells were suspended in soft agar and growth medium in 6-well plates at a density of 1,000 cells per well. After 2-3 weeks, colonies (≥10 cells) were counted under the microscope at five fields per well and photographed.

Migration and invasion assays. The migration assay was performed as described (Wong et al., 2005). The cell invasion assay was performed with self-coated Matrigel (BD Biosciences, San Jose, CA) on the upper surface of a transwell chamber. The invasive cells that had invaded through the extracellular matrix layer to the lower surface of the membrane were fixed with methanol and

stained with crystal violet. Photographs of three randomly selected fields of the fixed cells were captured and cells were counted. The experiments were repeated independently three times.

Annexin V staining. Cells were stained in binding buffer, 7-AAD and FITC-conjugated Annexin V as provided by the Annexin-V-FLUOS Staining Kit (Roche Diagnostics) according to manufacturer's instructions. Analysis was determined by a FACSCalibur flow cytometer and CellQuest software (BD Biosciences).

Single cell sorting. Viable $CD24^-$ and $CD24^+$ cells from a single cell suspension of PLC/PRF/5 were sorted into wells of a 96-well microtitre plate using a FACSAria cell-sorter equipped with an automated cell deposition unit (ACDU) and using 488-nm laser light. For single cell deposition, cells were sorted using the 70µm nozzle with the sheath pressure set at 70 PSI using the sort precision mode set at single cell. Dead cells were excluded from the sort based on their forward and side scatter characteristics using an electronic gate, before applying sort gates to define $CD24^+$ expressing cells for collection. The number of cells deposited in each well was one cell per well. Plates were maintained at 37°C in a humidified incubator with 5% CO2 in either physiologic oxygen (2–5%). Plates were manually screened and wells scored as positive if a cell colony was found. Selected colonies were expanded and used for future analysis.

Flow cytometric analysis. The antibodies used included phycoerythrin (PE)-conjugated CD24 (BD PharMingen, San Jose, CA), allophycocyanin (APC)-conjugated monoclonal mouse anti-human CD133/2 (Miltenyi Biotec, Aubum, CA), and fluorescein isothiocyanate (FITC)-conjugated monoclonal mouse anti-human epithelial antigen (DAKO, Carpentaria, CA). Cells were incubated in phosphate-buffered saline (PBS) containing 2% fetal bovine serum (FBS) and 0.1% sodium azide followed by PE, APC- or FITC-conjugated antibodies. Isotype-matched mouse immunoglobulins served as controls. The samples were analyzed using a FACSCalibur flow cytometer and CellQuest software (BD Biosciences, San Jose, CA).

Chromatin immunoprecipitation (ChIP) assay. The cells were processed for ChIP assays using Pierce Agarose ChIP kit (Thermo Fisher Scientific, Rockford, IL). Briefly, cells were cross-linked for 10 min with 1% formaldehyde and lysed. Lysate pellets were resuspended and sonicated with a Microson sonifier XL-2000 (Misonix). Protein-DNA complexes were immunoprecipitated using either phosphorylated Stat3 (Y705) antibody (Cell Signaling Technology Danvers, MA) or Normal rabbit IgG (Thermo Fisher Scientific, Rockford, IL) bound to protein A/G agarose, eluted, and

digested with proteinase K. For PCR analysis of the ChIP samples before amplicon generation, QIAquick-purified immunoprecipitates were dissolved in 50 µL of water. Standard PCR reactions using 3µL of the immunoprecipitated DNA were performed with a SYBR Green PCR kit (Applied Biosystems) using GPH1002937(-)17A (Superarray Bioscience, Frederick, MD) which generates a PCR amplicon centered 16381 base pairs upstream of the NM_024865.2 (Nanog) transcirption start site. Bioinformatics analysis is based on the Human Genome Build from the UCSC Genome Browser Feb. 2009 (GRCh37/hg19) Assembly. Calculation of pStat3 (Y705) occupancy on the *Nanog* promoter was performed according to the ChIP-qPCR primer assay data analysis template from Superarray Bioscience (Frederick, MD).

Quantitative PCR (qPCR) analysis. Total RNA was isolated using Trizol reagent according to the manufacturer's protocol (Invitrogen, Carlsbad, CA). Complementary DNA (cDNA) was synthesized using a GeneAmp® Gold RNA PCR Kit (Applied Biosystems, Foster City, CA) according to the manufacturer's instructions and then subjected to PCR with a SYBR Green PCR kit with primers the sequences of which are provided in Supplementary Methods. For single cell sorting experiment, RNA extraction and cDNA synthesis were carried out using the Power SYBR Green Cells-to-CT™-kit (Applied Biosystems), according to manufacturer's instructions. The amplification protocol consisted of incubations at 94°C for 15 seconds, 63°C for 30 seconds, and 72°C for 60 seconds. Incorporation of the SYBR Green dye into PCR products was monitored in real time with an ABI 7900HT Sequence Detection System and SDS 1.9.1 software (Applied Biosystems) and subsequently analyzed using RQ Manager 1.2 software (Applied Biosystems), thereby allowing the threshold cycle (C_T) at which exponential amplification of the products began to be determined. The amount of target cDNA was calculated relative to that of β-actin cDNA.

Western blot analysis. Western blots were developed using an ECL Plus kit (Amersham Biosciences, Piscataway, NJ). The primary antibodies included rabbit anti-human Nanog, anti-human Stat3 (79D7), phospho-Src (Y416), JAK2 (D2E12), phospho-JAK2 (Tyr1007/1008), mouse monoclonal XP rabbit anti-human phospho-Stat3 (Tyr705) (D3A7) (Cell Signaling Technology Danvers, MA), mouse anti-human CD90 (Abcam, Cambridge, MA) and mouse anti-human β-actin (Santa Cruz Technology, Santa Cruz, CA). After washing, the membrane was incubated with horseradish peroxidase–conjugated anti-mouse or rabbit or goat antibody (Amersham) and then visualized by enhanced chemiluminescence plus according to the manufacturer's protocol.

Immunostaining, immunofluorescence staining and histopathology. For paraffin-embedded

tissues, sections were deparaffinized in xylene and rehydrated in graded alcohols and distilled water. Slides were processed for antigen retrieval by a standard microwave heating technique. Specimens were incubated with goat anti-human CD24 (C-20) (Santa Cruz Biotechnology, Santa Cruz, CA) in a dilution of 1:100. Subsequent immunodetection was performed using the standard rapid EnVision technique. The reaction was then developed with the DAKO Liquid DAB_Substrate-Chromogen System (DAKO, Carpentaria, CA). Sections were counterstained with Mayer's hematoxylin. Stained slides were imaged on an Aperio Scanscope® CS imager (Vista, CA), generating 0.43 μm/pixel whole slide images. These images were compiled, and CD24 expression was quantitated using the Aperio Spectrum® software with a pixel count algorithm.

Immunofluorescence was performed on differentiating hepatospheres. First, floating hepatospheres were adhered onto chamber slides and differentiated in the presence of 10% FBS for 24 hours; subsequently they were fixed and permeabilized with 0.1% Triton X-100 and fixed with 4% paraformaldehyde in PBS. The cells were incubated with FITC-conjugated mouse anti-human CD24 (clone ML5) (1:100) (BD Pharmingen, San Jose, CA) and PE-conjugated monoclonal mouse anti-human Cytokeratin 18 (2X44) (Santa Cruz Biotechnology, Santa Cruz, CA), and subsequently counterstained with DAPI for 5 minutes at room temperature (AppliChem GmbH, Germany). All images were visualized under a fluorescent microscope.

For histological analysis, tissues were fixed in formalin, embedded in paraffin, cut into 4-μm sections and stained with hematoxylin and eosin stain as described (Lee et al., 2007).

Experimental metastasis model. A total of $1x10^4$ luciferase-labeled cells were suspended in 100μL of complete medium and then injected into the tail veins of NOD/SCID mice to enter into circulation. At 40 days after tumor injection, focus formation was inspected by xenogen imaging, observing either the whole anaesthetized mouse or the lungs that were removed immediately after sacrificing the mice. The lungs were then collected for paraffin embedding.

Pathway analysis. The Ingenuity Pathway Analysis Tool was used to examine the functional associations among genes and generate a gene network with high significance on the basis of more interconnected genes being present than would be expected by chance. The significance of each network was estimated by the scoring system provided by Ingenuity. The scores were determined by the number of differentially expressed genes within each of the networks and the strength of the associations among network members. Once over-represented genes that are functionally relevant

in the gene networks were identified, we validated their functional association by using the independent pathway analysis tool PathwayAssist (Version 3.0, Ariadne Genomics).

Primer sequences for qPCR analyses.

Gene	*Forward primer (5'-3')*	*Reverse primer (5'-3')*	*GenBank No.*
CD24	TGAAGAACATGTGAGAGGTTTGAC	GAAAACTGAATCTCCATTCCACAA	NM_013230
CK18	TCT CCCCGGACAGCATGA	CCGGTAGTTGGTGGAGAA	NM_000224
β-actin	CATCCACGAAACTACCTTCAACTCC	GAGCCGCCGATCCACACG	NM_001101
β-catenin	ACAACTGTTTTGAAAATCCA	CGAGTCATTGCATACTGTCC	NM_001098209
Nanog	AATACCTCAGCCTCCAGCAGATG	TGCGTCACACCATTGCTATTCTTC	NM_024865
Notch1	CCTGAGGGCTTCAAAGTGTC	CGGAACTTCTTGGTCTCCAG	NM_017617
Oct4	CTTGCTGCAGAAGTGGGTGGAGGAA	CTGCAGTGTGGGTTTCGGGCA	NM_002701
Sox2	AAATGGGAGGGGTGCAAAAGAGGAG	CAGCTGTCATTTGCTGTGGGTGATG	NM_003106
Bmi-1	TGGAGAAGGAATGGTCCACTTC	GTGAGGAAACTGTGGATGAGGA	NM_005180
Smo	TGGTCACTCCCCTTTGTCCTCAC	GCACGGTATCGGTAGTTCTTGTAGC	NM_005631
Nestin	CTGCGGGCTACTGAAAAGTT	AGGCTGAGGGACATCTTGAG	NM_006617
ABCG2	TCATCAGCCTCGATATTCCATCT	GGCCCGTGGAACATAAGTCTT	NM_004827
ABCB1	AAATTGGCTTGACAAGTTGTATATGG	CACCAGCATCATGAGAGGAAGTC	NM_000927
ABCB5	TCTGGCCCCTCAAACCTCACC	TTTCATACCGCCACTGCCAACTC	NM_178559
ABCC1	CTCCTCCTATAGTGGGGACATCAG	GTAGTCCCAGTACACGGAAAG	NM_004996
ABCC2	ATGCAGCCTCCATAACCATGA	CTTCGTCTTCCTTCAGGCTATTCA	NM_000392

Short-hairpin RNA sequences.

Gene (sequence number)	*Sequence*
CD24 (278)	cd24-sh1-CCGGTCTTCTGCATCTCTACTCTTACTCGAGTAAGAGTAGAGATGCAGAAGATTTTTG
CD24 (121)	cd24-sh2- CCGGCGCAGATTTATTCCAGTGAAACTCGAGTTTCACTGGAATAAATCTGCGTTTTTG
CD90	cd90-sh-CCGGCGAACCAACTTCACCAGCAAACTCGAGTTTGCTGGTGAAGTTGGTTCGTTTTTG
Non-target control	CCGGTTGTGCTCTTCATCTTGTTGCCGGCAACAAGATGAAGAGCACCAATTTTTG

Supplemental References

Brown, J.J., Parashar, B., Moshage, H., Tanaka, K.E., Engelhardt, D., Rabbani, E., Roy-Chowdhury, N., and Roy-Chowdhury, J. (2000). A long-term hepatitis B viremia model generated by transplanting nontumorigenic immortalized human hepatocytes in Rag-2-deficient mice. Hepatology *31*, 173-181.

Lee, T.K., Poon, R.T., Guan, X.Y., Ma, S., Guan, X.Y., Myers, J.N., Altevogt, P., and Yuen, A.P. (2007). Lupeol suppresses cisplatin induced NFκB activation in HNSCC cells and inhibits local invasion and nodal metastasis in orthotopic nude mouse model of tongue squamous cell carcinoma. Cancer Res. *67*, 8800-8809.

Li, Y., Tang, Z.Y., Ye, S.L., Liu, Y., Chen, J., Xue, Q., Huang, X., Chen, J., Bao, W., and Yang, J., et al. (2001). Establishment of cell clones with different metastatic potential from the metastatic hepatocellular carcinoma cell line MHCC97. World J. Gastroenterol. *7*, 630-636.

Ng, I.O., Liang, Z.D., Cao, L., and Lee, T.K. (2000). DLC-1 is deleted in primary hepatocellular carcinoma and exerts inhibitory effects on the proliferation of hepatoma cell lines deleted DLC-1. Cancer Res. *60*, 6581-6584.

Wong, C.M., Yam, J.W., Ching, Y.P., Yau, T.O., Leung, T.H., Jin, D.Y., and Ng, I.O. (2005). Rho GTPase-activating protein deleted in liver cancer suppresses cell proliferation and invasion in hepatocellular carcinoma. Cancer Res. *65*, 8861-8868.